
**Instituto Politécnico de Lisboa**

**Instituto Superior de Engenharia de Lisboa**

**Escola Superior de Tecnologia da Saúde de Lisboa**

# Inertial-sensor based 3D kinematics in the differential diagnosis between Parkinson's disease and atypical parkinsonism

**Pedro Correia Ferreira**

Thesis to obtain the Master's Degree in

## Biomedical Engineering

**Supervisors:** Marcelo Mendonça (Centro Hospitalar de Lisboa Ocidental)
Pedro Mendes Jorge (ISEL)

## Examination Committee

**Chairperson:**
João Costa, PhD, ISEL

**Members of the Committee:**
Miguel Coelho, PhD, Centro Hospitalar de Lisboa Norte; Faculdade de Medicina, Universidade de Lisboa
Marcelo Mendonça, PhD, Centro Hospitalar de Lisboa Ocidental

## Final version

December 2019


Fundação
Champalimaud

# Inertial-sensor based 3D kinematics in the differential diagnosis between Parkinson's disease and atypical parkinsonism

**Pedro Correia Ferreira**

This work was developed at Hospital Egas Moniz, Centro Hospitalar de Lisboa Ocidental, and at the Neurobiology of Action Lab in Fundação Champalimaud, Champalimaud Center for the Unknown, under the supervision of Marcelo Mendonça, MD, and Pedro Mendes Jorge, PhD, for obtention of the master's degree in biomedical engineering from Instituto Superior de Engenharia de Lisboa (ISEL) and Escola Superior de Tecnologia da Saúde (ESTeSL).

## Acknowledgments

I would like to thank my supervisors, Marcelo Mendonça and Pedro Mendes Jorge, for their unconditional support and availability whenever I needed help. I would have never been able to achieve this without their persistence, knowledge and insight.

I would also like to thank professor Cecília Calado for her counseling, and together with the teaching team, for the tools they provided me with during this master's degree, which were fundamental.

Also, I would like to express my gratitude to Bruna Meira and Raquel Barbosa from the neurology team at CHLO, for their assistance with patient recruitment and data collecting, and to Ricardo Matias and Ana Clemente from Kinetikos, for their data acquisition support and training, and aiding with data processing.

Thank you Rui Costa, and the team from the Neurobiology of Action Lab at the Champalimaud Foundation for the opportunity of accessing and working on a science focused environment, which gave me a new perspective on the research working reality.

Finally, a special thanks should be given to my family, especially my parents José and Clara Ferreira, and my girlfriend, Sandrine Martins, for this wouldn't have been possible without their continuous support and patient throughout this journey.

## Abstract

**Background and Objectives:** Parkinson's disease (PD) is the most frequent disorder presenting with Parkinsonism. However, atypical parkinsonian disorders (such as Progressive Supranuclear Palsy (PSP) and Multiple System Atrophy (MSA)) share some clinical features of PD but have different prognosis and are therefore important to distinguish from PD. The development of new and cost-effective tools to help clinicians in the differential diagnosis is therefore paramount. In this work, we perform sensor based kinematic analysis to find significant differences between PD and atypical parkinsonism, while developing an experimental machine learning model with clinical applicability.

**Subjects and Methods:** 32 subjects with PD (mean age 69.7 ± 11.3, 14 male 17 female), 11 with atypical parkinsonism (9 PSP, 1 MSA, 1 vascular parkinsonism, mean age 72.9 ± 6.1, 8 male 3 female) and 33 age-gender matched controls (mean age 68.0 ± 12.6, 14 male 19 female) were recruited from the outpatient clinic in routine appointments at Hospital Egas Moniz, Lisboa. Using a set of 7 inertial sensors, leveraged by biomechanical models, we collected data from gait and posture during a 3x20m walk and stance. Moreover, using one inertial sensor, we recorded finger tapping tests. We conducted the analysis in two different ways: controls vs parkinsonian group (ill – PD + atypical), and within the parkinsonian group i.e. PD vs atypical.

**Results:** Compared to controls, parkinsonian subjects displayed lower cadence (controls 109.420 ± 12.519 steps/min, ill 100.566 ± 13.432 steps/min, $p = 0.006$), step length (controls 0.512 ± 0.086 m, ill 0.442 ± 0.100 m, $p = 0.003$) and speed (controls 0.996 ± 0.190 m/s, ill 0.773 ± 0.202 m/s, $p < 0.001$). Double support was increased in the parkinsonian cohort (controls 36.355 ± 3.253 %, ill 39.827 ± 5.685 %, $p = 0.003$), and angular variables were decreased for the most part (i.e. hip flexion mean velocity controls 67.900 ± 14.974 cm/s, ill 55.180 ± 12.814 cm/s, $p<0.001$). A 10-fold cross validation random forest model classified controls vs parkinsonian subjects with an accuracy of 82.9%.

PD and atypical cohorts also differed significantly, with the latter displaying high asymmetry in many angular parameters: knee mean velocity asymmetry (PD 0.919 ± 0.710 cm/s, atypical 3.392 ± 3.836 cm/s, $p = 0.001$), hip adduction mean velocity asymmetry (PD 0.268 ± 0.177 cm/s, atypical 0.656 ± 0.563 cm/s, $p = 0.002$) and ankle mean velocity asymmetry (PD 0.636 ± 0.537 cm/s, atypical 1.586 ± 1.227 cm/s, $p = 0.002$). The same machine learning model classified the PD vs atypical cohorts with 76.3% accuracy.

Ongoing work is being developed in the analysis of finger tapping and postural metrics that can improve the discrimination models.

**Conclusions:** The main objectives of this work were achieved. We hypothesize that atypical parkinsonian subjects develop an instable gait where asymmetry is highly pronounced compared to PD. Furthermore, we believe inertial sensor technology supported by machine learning should become a regularly applied technique in the differential diagnosis of these syndromes.



**Keywords:** Parkinson's disease; Atypical parkinsonism; Differential diagnosis; Sensor-based kinematic analysis; Applied machine learning.

## Table of Contents

## List of Figures

## List of Tables

## 1. Introduction

Parkinson's disease is the second most prevalent neurodegenerative disorder worldwide, and even though it represents the most typical form of parkinsonism (marked by bradykinesia, postural instability, tremor and rigidity), it's mimicked by other syndromes, commonly termed as atypical parkinsonism [1]. Of these, the most common are Progressive Supranuclear Palsy, Multiple System Atrophy and Vascular Parkinsonism, and despite each one having particular clinical features, at an early stage, these can easily be mistaken for Parkinson's disease. Although some diagnostic techniques such as MRI [2], tau-PET [3] and DaTscan [4] play a role in distinguishing between Parkinson's disease and atypical parkinsonism, these methods are not only expensive and out of reach for a large part of the population (for they are only available at specialized clinic centers), but also no technique is yet fully effective in the differential diagnosis. This way, Parkinson's disease and atypical parkinsonian syndromes represent slow progressing neurodegenerative disorders that can manifest in a broad range of symptoms, each one having different treatments and prognostics, therefore becoming necessary to develop new, cheaper and more accessible techniques that can be applied on every day clinical practice to aid the differential diagnosis.

The use of inertial sensors to assess gait characteristics in patients with movement disorders has recently seen an increase, but these are not yet used in clinical context [5]. Furthermore, several studies have tried to quantify gait in Parkinson's disease, but number of sensors, positioning and relevant spatiotemporal kinematic parameters still suffer from high variability and thus an optimal approach is still to be developed before inertial sensors make their way into clinical practice [5]. In addition, quantification of gait in subjects with atypical parkinsonism has seen far less research, making it a field where much is still to be found. In this work a 3D full body kinematics model will be used in order to assess gait in Parkinson's disease and atypical parkinsonism where a broad range of spatiotemporal kinematic parameters will be collected in order to best quantify gait. These will be composed of traditional spatiotemporal parameters such as speed and gaits' phases, but also angular, non-linear parameters and asymmetry.

The focus of this work will be to primarily find statistically significant spatiotemporal parameters that can distinguish between Parkinson's disease and atypical parkinsonism. This will be done in two levels: firstly, PD and atypical subjects will be merged in the same group and compared to controls; then, PD and atypical cohorts will be individually compared for significant differences. Afterwards, kinematic parameters will be correlated with patients' clinical data such as disease duration and motor-UPDRS, to see if inertial sensors can be used as a tool to measure patients' condition. Finally, an experimental machine learning model will be constructed in order to try and classify Parkinson's disease and atypical parkinsonism subjects. Can inertial sensors be used in the differential diagnosis between Parkinson's disease and atypical parkinsonism? Which are the most significant differences in gait between these two cohorts? How do they compare to controls? Can machine learning be used as a tool to help common clinical practice in diagnosing these syndromes? These are all questions that will be tackled during this work.

## 2. Parkinson's Disease

Now over two hundred years ago, James Parkinson made the first approach to clinically describe a syndrome he called "shaking palsy" in his 1817 "An essay on the shaking palsy" as "*Involuntary tremulous motion, with lessened muscular power […] with a propensity to bend the trunk forward, and to pass from a walking to a running pace*" [6]. Later that century, Jean-Martin Charcot credited J. Parkinson by suggesting the name "Parkinson's Disease", while more carefully describing the disease, distinguishing some of its features and its clinical spectrum, and differentiating between two variations: the tremulous and the rigid/akinetic form [7]. Since these first descriptions, Parkinson's Disease (PD) has been widely studied and can be succinctly described as a complex, multisystem neurodegenerative disorder characterized by the loss of dopaminergic neurons in the substantia nigra pars compacta [1], and while dopamine deficiency is its hallmark and responsible for the characteristic motor symptoms, many other neurotransmitters are affected, such as acetylcholine, serotonin and noradrenaline [8]. It is suggested that the degeneration of these neurotransmitters is responsible for the non-motor symptoms, which can precede the motor ones for more than a decade - also called, the prodromal phase. Treatment heavily relies on pharmacological therapy that increase dopamine concentration, and unlike previous beliefs that Parkinson's Disease was primarily caused by environmental factors, research is now revealing that the disease might be the result of a network interplay between genetics and the environment [1]. Associated with the diagnostic challenges which mainly remain clinical and susceptible to human error, Parkinson's Disease represents a slowly progressive neurodegenerative disorder that can manifest in a broad array of symptoms, affecting a multitude of neuroanatomical areas and without a chance of early diagnosis.

### 2.1. Risk Factors & Genetics

Parkinson's Disease affects an estimated 10 million people worldwide and about 1-3% of the population over 60 years old [9]; demographically, it appears to have higher incidence in Europe, North and South America when compared to Asian, Arabic and African countries [1], and ethnically, from the highest to the lowest affected ethnicity, it affects Hispanics, non-Hispanic Whites, Asians and Blacks [10]. Men are more affected by the condition when compared to women with a ratio of 3:2 [11], but the greatest risk factor for Parkinson's Disease is age, with its prevalence increasing exponentially at 80 years old [12]. Although all the above-mentioned factors play a role in the risk of developing Parkinson's Disease, many other factors must be taken into consideration. First, we must understand the two forms in which PD can develop: familial and idiopathic. Familial Parkinson is genetically inherited in either an autosomal dominant or recessive manner [13], while idiopathic Parkinson develops from gene-environment interactions [14][15]. The latter accounts for about 85% of all PD cases, and due to the fact that the human genotype is unique from individual to individual, similar exposures to the same environmental factors affect individuals in different ways and may result in different disease phenotypes [15]. For a better understanding of how gene-environment factors can affect the propensity of developing PD, caffeine is an adenosine A2A (gene ADORA2A) receptor antagonist that increases dopaminergic neurotransmission, which suggests that polymorphisms in this gene may correlate higher coffee consumption to lower PD risk [16]. On the other hand, heavy metals contribute positively to the risk of developing PD as shown in several previous studies: for instance, iron contributes to neuronal death through the generation of oxidative stress; similar to iron, high concentrations of copper in the brain leads

to the reduction of dopamine and neuronal protective factor, with the increase of alpha-synuclein aggregates [15].

### 2.2. Pathology & Pathogenesis

Before going into Parkinson's Disease pathology itself, it is possible to use its simplest pathological description to understand the underlying neurological mechanisms behind it - therefore, it can be succinctly described as the loss of dopaminergic neurons within the substantia nigra pars compacta (SNpc). The SNpc is found within the basal ganglia, which are a group of subcortical structures found at the base of the forebrain and top of the midbrain. The forebrain section is composed of the caudate nucleus, putamen, nucleus accumbens and globus pallidus that together make up the striatum, while the midbrain section is composed of the subthalamic nucleus and the substantia nigra. The latter is divided into two parts: the pars compacta and the pars reticulata. For a better understanding of these structures, refer to figures 1 and 2 which represent sagittal and coronal planes of the basal ganglia, respectively.

The basal ganglia play an important role in movement control and are responsible for processing signals from the cortex, reaching it from the caudate nucleus and the putamen (input structures). In contrast, the output structures are mainly the substantia nigra and the globus pallidus, sending projections to the cortex through the thalamus. The way basal ganglia process signals from the cortex can be described by two distinct pathways: the direct pathway and indirect pathway. The two pathways have opposite effects when it comes to their output: the direct pathway excites thalamic neurons which in turn excite cortical neurons, while the indirect pathway inhibits thalamic neurons which are then unable to excite cortical neurons; that said, it is believed that normal functioning of the basal ganglia is dependent on the balance between the activity of both, and, therefore, complications in one of them can result in incorrect movement control [17]. Parkinson's Disease is exactly that: the loss of dopaminergic neurons within the SNpc causes disruption in an important dopaminergic pathway, which leads to most of the motor symptoms seen in PD patients, like bradykinesia, rigidity, and the overall motor fluctuations, which will all be discussed later during this work [1].

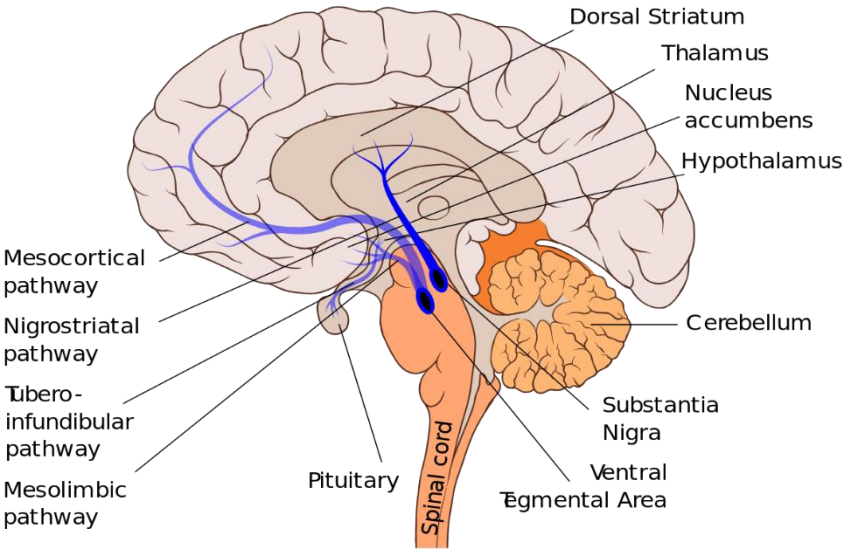


**Figure 1** - Sagittal representation of the basal ganglia

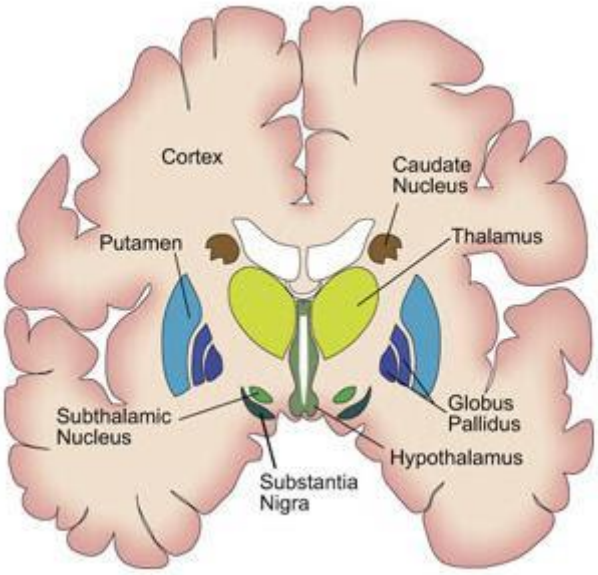


**Figure 2** - Coronal representation of the basal ganglia

Another pathological feature of PD, and one of the most widely studied [18], is Lewy pathology. In 1997, a genetically inherited dominant form of PD was correlated with a mutation in the SNCA gene, which encodes α-synuclein [19]. In its native state, α-synuclein is unfolded, but in the presence of negatively charged lipids it folds into amphipathic α-helices [18] and becomes insoluble, aggregating and forming intracellular inclusions within nerve cells, called Lewy bodies; these may also develop along axons and dendrites (together called neurites), in which case are called Lewy neurites [1]. Morphologically, these aggregates typically have a length of 50-700nm and a width of 5-10nm [20], and can develop not only in the brain but also the spinal cord and peripheral nervous system, and for most idiopathic PD cases, development of these structures can be described in a standardized pattern by the Braak 6-stage model [21].

The Braak model 1st stage points to the presence of α-synuclein aggregates in the olfactory structures and the dorsal motor nucleus of the vagus nerve, possibly leading to the

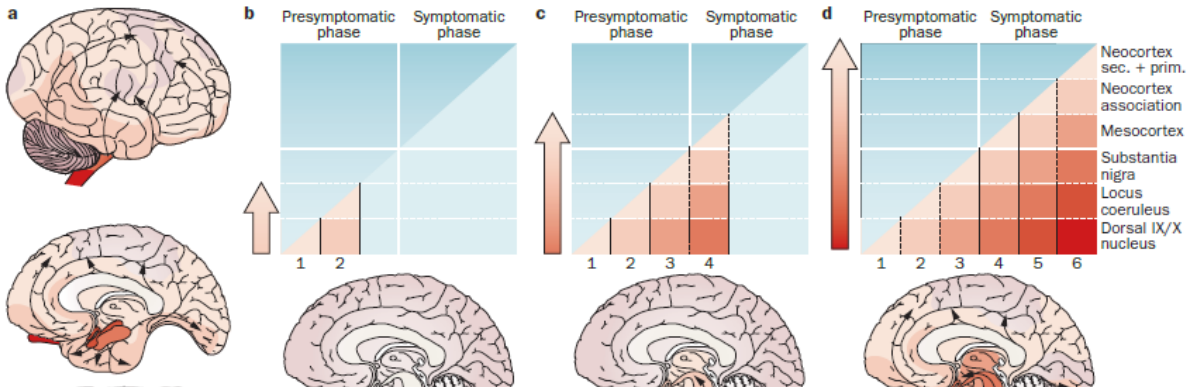


**Figure 3** - Six stages of the Braak model. b) Stage 1 and 2 affecting the olfactory structures and the dorsal motor nucleus of the vagus nerve. c) Stages 3 and 4 reaching the substantia nigra pars compacta and the anteromedial temporal mesocortex. d) Stages 5 and 6 with inclusions spreading to high order and first order sensory association areas of the neocortex. Adapted from Goedert et al., 2012.

onset of the prodromal phase where olfactory impairments and autonomic regulatory disfunctions can be visible. In stage 2, Lewy pathology will develop in the medulla oblongata and the pontine tegmentum. The substantia nigra sees the arrival of Lewy bodies at stage 3, which during this time motor symptoms like bradykinesia, tremor, gait disturbance or rigidity will become visible. The 4$^{th}$ stage is marked by the appearance of α-synuclein aggregates in the anteromedial temporal mesocortex. At stage 5 inclusions reach the high order sensory association areas of the neocortex, and at stage 6 the first order sensory association areas and motor fields – it is at this point that most of the advanced cognitive symptoms of PD become evident [18], [21]. Figure 3 visually represents the development and evolution of Lewy pathology in the brain of PD patients according to the Braak model.

Lewy pathology seems to have a strong correlation with non-motor symptoms of PD, particularly cognitive impairment and eventually dementia. Parkinson's disease dementia (PDD) commonly develops in advanced cases of PD and its diagnosis is carried out when cognitive impairment is visible in long lasting idiopathic PD [18]. Lastly, even though the Braak staging model of Lewy pathology seems to apply to a large number of PD cases, it doesn't apply to all, thus, further studies are necessary [1].

Taking into consideration the abovementioned, there have been important findings that show Parkinson's disease is more than a correlation between neurodegeneration and Lewy pathology alone. First, α-synuclein not only aggregates into Lewy bodies and neurites, but also form different structures [1] of which, some, like oligomers, might be toxic to neurons [22]. Furthermore, in some cases, other protein aggregations are found within the brains of PD patients, like β-amyloid plaques and tau neurofibrillary tangles, which are commonly found in Alzheimer's disease; as a matter of fact, up to 50% of PD patients with PDD are prone to develop Alzheimer's disease at some point [23], which might be an indicator that along with Lewy pathology, other protein aggregations may play a significant role in neurodegeneration. It's also important to mention that Lewy pathology does not occur in all PD cases, particularly in a large proportion of PD related to *parkin* and LRRK2 gene mutations [1].

Lastly, neuroinflammation has also been subject of study as a pathological feature of PD. Epidemiological studies have shown a reduced risk of PD development with intake of anti-inflammatory drugs, and even though it's not yet known which role neuroinflammation plays (whether promotive or protective), studies like this might be illusive in this matter [24]. Furthermore, studies using calcium channel blockers and serum urate have been conducted to assess their effect in neuronal oxidative stress, and showed a reduced risk for PD development. SNpc neurons are susceptible to high levels of mitochondrial oxidative stress due to high intracellular calcium influx, and thus, calcium channel blockers and serum urate (an antioxidant) might have the ability to protect neurons from oxidative stress.

### 2.3. Clinical Features

Parkinson's disease can be described by four, well established clinical features: rest tremor, rigidity, postural instability and akinesia (or bradykinesia); these will be exhaustively described in the following sections. The heterogenicity of these symptoms spurred the need to classify different subtypes of the disease, and so far, two major subtypes are widely accepted: tremor dominant (TD) PD and non-tremor dominant PD – the latter usually divided into two phenotypes: the akinetic-rigid syndrome (AR) and the postural instability gait disorder (PIGD).

Finally, an additional subgroup of PD patients has an indeterminate or mixed disease subtype. How to distinguish the different disease subgroups and phenotypes will be later discussed since differentiating between them will be relevant to this study.

1. **Rest tremor**

Although not present in all PD cases, rest tremor is one of the most common and easy to recognize motor features of PD. Prominently involving the distal part of an extremity (usually the hands), it can also affect the legs, chin, jaw and lips, occurs unilaterally at a frequency of 4-6Hz [25] and is best observed when patients are asked to rest their hands on the lap. Interestingly, its effect can be reduced with mental distraction, such as when the patient is asked to count backwards [26]. As the term suggests, rest tremor tends to disappear with action. Furthermore, patients with PD may also experience postural tremor, which occurs when maintaining a position against gravity [27]. Rest tremor and postural tremor (characteristic of PD) are not to be mistaken with essential tremor (a common movement disorder), and there are various features than can distinguish between both (see table 1). Finally, and as mentioned before, studies suggest that a proportion of patients (11-30%) don't show signs of tremor during disease [25].

**Table 1** - Features differentiating PD rest and postural tremor from Essential tremor. Adapted from [25].

| Features | PD | Essential tremor |
|---|---|---|
| **Age at onset** | 55-75 | 10-80 |
| **Tremor frequency [Hz]** | 4-6 | 5-10 |
| **Tremor characteristics** | Supination - Pronation | Flexion - Extension |
| **Limb tremor** | Asymmetric | Symmetric |
| **Distribution** | Face, jaw, lips, chin | Head, voice |

2. **Bradykinesia**

Bradykinesia is defined as "slowness of initiation of voluntary movement with progressive reduction in speed and amplitude of repetitive actions" by the Queen Square Brain Bank diagnostic criterion of PD. Patients not only find it hard to initiate and execute movements but may also present decrease reaction times and blinking, loss of spontaneous movements, hypomimia (loss of facial expression) and reduced unilateral arm swing [25]. Along with tremor it is one of the easiest to recognize features of PD. It's usually observed during a neurology appointment when patients are asked to perform repetitive movements like finger taps, heel and toe taps and hand pronation-supination movements, with the clinician assessing not only slow movements but also amplitude reduction. It is believed that bradykinesia is the result of dopaminergic deficiency that leads to the disruption of normal motor cortex activity, affecting various cortical and subcortical structures [25].

3. **Postural instability**

Postural instability is the most common cause of falls and generally manifests only at late stages of PD, differentiating it from PSP and MSA, the other two neurogenerative disorders that will be discussed during this work. It's assessed with the pull test, where the clinician pulls the patient backwards applying force on the shoulders, and observing the retropulsion response. Taking more than two steps backwards or lack of postural response suggests a considerable level of postural instability [25]. For comparison, a 2005 study showed that the time between symptoms onset to the first fall was, on average, 16.8 months for Progressive Supranuclear Palsy, 42 months for Multiple System Atrophy (disorders which will both be described later), and 108 months for PD [28].

4. **Rigidity**

Rigidity is characterized as a continuous increase of muscle tone which is felt as constant resistance associated with passive limb movements around a joint, and can be assessed when the clinician actively moves the patients' limb in an extension, flexion or rotation movement [25]. So called "reinforcing manoeuvres" or Froment's manoeuvre, which is the voluntary movement of a contralateral body part, can increase this rigidity [29], and becomes perceptible when the clinician is, for example, actively flexing/extending the patients right forearm and asks the patient to rotate his left wrist. Rigidity in particular body structures may also lead to abnormal axial postures, like in the cases where the patient displays a flexed neck or trunk, however, these deformities usually only appear at advanced stages of the disease [25].

## 2.4. Diagnosis

Diagnosis of PD mainly remains clinical and focused on the clinical motor features that were already discussed, although, there is no definitive, optimal way of assessing it. The Movement Disorder Society (MDS) criteria for the diagnostic of PD is often used in daily practice to help make a clinical decision, and is based on both supportive and exclusion criteria, presented on table 2. Additionally to the analysis of this criteria, some rules must also be taken into consideration [8]:

1. Not all PD patients present tremor, so tremor is not needed for the diagnosis of PD;
2. Due to the other parkinsonian syndromes, presence of parkinsonism does not necessarily imply a diagnosis of PD;
3. Atypical features (such as early falls, early cognitive decline or poor response to medication, etc.) should be an indicator of other parkinsonian syndromes.

**Table 2** - Supportive and exclusion criteria for the diagnosis of Parkinson's disease; adapted from the Movement Disorder Society (MDS) clinical diagnostic criteria for PD.

| Supportive criteria | Exclusion criteria |
|---|---|
| Clear beneficial response to dopaminergic therapy | Absence of response to high-dose levodopa therapy despite at least moderate severity of disease |
| Presence of levodopa-induced dyskinesia | Parkinsonian features restricted to the lower limbs for at least 3 years |

| | |
|---|---|
| Presence of tremor of at least one limb (at 4-6 Hz), either during current or past examinations | Normal functional imaging of the presynaptic dopaminergic system |
| Presence of olfactory loss or cardiac sympathetic denervation on MIBG scintigraphy | Presence of cerebellar abnormalities such as cerebellar gait, limb ataxia or oculomotor abnormalities |
| For a concise PD diagnosis, supportive criteria must also include bradykinesia plus rest tremor or rigidity | Presence of any of the exclusion criteria must rule out PD |

In order to help clinicians diagnose and keep track of the clinical data and PD evolution of a patient, the MDS-UPDRS clinical rating scale for Parkinson's disease is commonly used, featuring four parts: 1. Non-motor experiences of daily living; 2. Motor experiences of daily living; 3. Motor examination; 4. Motor complications [30]. A number of questions are filled in by the examiner, giving a better perspective of the overall condition of a patient.

When patients present classical features that are common to PD, diagnosis is straightforward, although, in the early onset of disease, some symptoms can overlap with other syndromes, increasing the difficulty of the differential diagnosis - studies suggest that up to 20% of diagnosed PD cases end up with a different diagnosis at autopsy [26]. Some of the mimicking syndromes, also called parkinsonian syndromes (PS) or atypical parkinsonisms, are multiple system atrophy (MSA), progressive supranuclear palsy (PSP) and vascular parkinsonism, but other conditions can also lead to an uncertain diagnostic, such as essential tremor.

Various imaging techniques are assessed to help in the differential diagnosis between PD and its syndromes, such as positron emission tomography (PET) and single photon emission computed tomography (SPECT), the latter commonly associated with 123I-Ioflupane, also termed DaTscan [4]. This technique can help differentiating PSs from other disorders that present no loss of dopaminergic neurons in the SNpc (such as essential tremor), although, it cannot distinguish PD and the remaining parkinsonian syndromes [1].

## 3. Atypical Parkinsonisms

To understand the need for accurate differential diagnosis between Parkinson's disease and atypical parkinsonisms, it's important to comprehend not only where these syndromes differ from one another, but where they are similar and where mistakes can be made during diagnosis. Of all the atypical parkinsonian forms, this section will clarify important clinical data related to Progressive Supranuclear Palsy, Multiple System Atrophy and Vascular Parkinsonism.

### 3.1. Progressive Supranuclear Palsy

#### 3.1.1. Overview

The first form of atypical parkinsonism that will be discussed in this work is Progressive Supranuclear Palsy (PSP). Several studies estimate that its prevalence varies from 1.4 to 6.5 cases per 100000 person-years [31], and is considered a tauopathy - meaning that its principal neuropathological mechanism implies the deposition of aggregates of abnormal tau protein in neurons and glial cells of certain neuroanatomical areas, such as the brainstem and basal ganglia [32]. These aggregates are composed of filaments and tubules with four repeats of the microtubule-binding domain tau isoform (4R-tau), making PSP a 4R-tauopathy [31]. But which role does tau play in neurodegeneration? Normal tau is produced by neurons and helps with polymerization of neuronal microtubules, but it's thought that some tau isoforms are unsuccessful in this process, where, along with tau aggregates, makes this protein toxic [33]. Notoriously, the prion-like properties of tau have also been exposed, where abnormal tau isoforms have the ability to spread to non-affected areas of the brain and induce the formation of tau aggregates. Although these mechanisms are not yet clear, the prion-like feature of tau was observed in several in-vivo studies [31].

The Richardson's syndrome (RS) was the first phenotype to describe the classic behaviour of PSP, although, there are many more phenotypes like PSP-CBD (with corticobasal degeneration), PSP with progressive gait freezing (PSP-PGF) and PSP-P, the one that relates to PD the most, only first described in 2005 [34] and where many of its clinical features overlap with the ones seen in PD, such as asymmetric bradykinesia and rigidity, impaired postural reflexes and cognitive impairment. Some symptoms, like early postural instability, falls, and vertical supranuclear gaze palsy might help in the diagnosis of PSP, however, only as the disease progresses is it possible to make an objective decision. Hypokinesia without decrement seen in repetitive finger tap movements may also be a solid hallmark for the detection of PSP [35], but unfortunately, like PD, a definitive diagnosis can only be carried out post-mortem, and the majority of PSP cases are incorrectly diagnosed at the early onset of disease [31], with PD being its most common misdiagnosis; therefore, search for differential diagnostic features is paramount and could help with the prognostic of PSP cases.

#### 3.1.2. Diagnostic Tools

Neuroimaging techniques are usually the go-to tools for assessment of PSP, of which MRI and tau-PET seem to be the most promising thus far. MRI data consists of measuring the midbrain and superior cerebellar peduncle atrophy and the midbrain-pons area as clinical biomarkers for the RS phenotype, where this phenotype is discriminated from PD and MSA-P with very high specificity and sensitivity, both between 90-100% in many studies [2]; however,

other phenotypes are not so well discriminated [31][36]. On the other hand, tau-PET has shown promising results, with studies showing that the distribution of tau-radioligands in the brain corresponds to the areas where tau neurodegeneration is expected in PSP. For instance, uptake of tau radioligand 18F-AV1451 has been compared in PSP vs PD groups, and its distribution in the globus pallidus rendered the best discriminatory results, with 72.7% sensitivity and 93.5% specificity [3].

Other diagnostic tools include the evaluation of neurofilament light chain (NfL) associated with cerebrospinal fluid (CSF) as a potential neurological disease biomarker. CSF NfL releases into the blood stream when axonal damage is present, and higher concentrations are found in PSP and atypical parkinsonisms when compared to PD and controls, making it possible to differentiate between these – although, since NfL release is independent of cause and may result from different pathological mechanisms, it cannot distinguish between atypical parkinsonian syndromes alone [37]. Also, this procedure is done through lumbar puncture, a very invasive procedure that is not feasible to perform every time a differential diagnosis is required.

Interpretation of these factors reveal that even though progress is being made in order to assess PSP and its phenotypes, no technique is, so far, able to effectively differentiate between PD and PSP-P, RS and its' other phenotypes; neuroimaging fails to do so because it can only accurately identify PSP-RS, and the approach of measuring CSF NfL in blood shows promising results in differentiating PD from atypical parkinsonisms, but not between the latter.

## 3.2. Multiple System Atrophy

### 3.2.1. Overview

Another atypical parkinsonian syndrome that is important to be considered is Multiple System Atrophy (MSA). Prevalence of this disorder is estimated to be between 1.9 to 4.9 per 100000 person-years, but can be as high as 12 per 100000 after 70 years of age [38]. Along with PD and dementia with Lewy Bodies, it's considered an alpha-synucleinopathy, meaning that it's characterized by accumulation of abnormal fibrillary alpha-synuclein, the same inclusions that were already discussed in pathology and pathogenesis of PD. In the case of MSA, these inclusions form in the oligodendroglia (a type of neuroglia that provide support to axons), making it one of the pathological hallmarks of the disease [39]. Depending on how it manifests, it can be divided into two phenotypes: the parkinsonian variant due to striatonigral degeneration (MSA-P) and the cerebellar variant (MSA-C). According to different studies, western populations are more affected by the MSA-P variant (70-80%), whilst the MSA-C variant seems to have higher incidence in Asian populations (67-84%) [38]. The MSA brain may present atrophies in several neuroanatomical regions, namely in the cortex frontal lobes, cerebellum and pontine base. Atrophies range from various levels of severity, but the presence of astroglial cytoplasmic inclusions (GCI) is one of the features required for the post-mortem diagnosis of MSA; in fact, these are responsible for most of the reported neurodegeneration, affecting a broad range of systems and structures [38].

Like PSP, MSA shares many of its clinical features with PD, being mostly characterized by rigidity, bradykinesia, rapid eye movement (REM) sleep disorder, autonomic dysfunction and postural instability, but shows poor response to levodopa treatment as well as minimal signs of rest tremor. Still, some features are different between PD and PSP, mainly between

its MSA-C phenotype, for its clinical presentation differs in a few aspects, like cerebellar ataxia, early and severe dysphagia, etc. [38], although, the early onset of disease can become a confusing state with various overlapping features, leading to a misdiagnose. As a matter of fact, since a definitive MSA diagnostic can only be conducted post-mortem, a study showed that only 62% of MSA cases diagnosed during life were confirmed after autopsy [40].

### 3.2.2. Diagnostic Tools

Like PD, MSA diagnosis remains clinical for the most part, but also possesses other diagnostic tools. Of these, neuroimaging provides good results for assessment of MSA, because currently there are no fluid biomarkers that can reliably aid in its diagnosis [38]. Now, when it comes to neuroimaging techniques there's a large number of approaches that try to distinguish between MSA and Parkinson's disease, of which, the following should be noted:

1. MIBG scintigraphy scan can help differentiate MSA-P from PD with a specificity of 77% [41];
2. Through MRI, values of mean diffusion volumes of the putamen in MSA-P is higher compared to PD, and an extensive brain volume loss is visible in MSA-P, but not in PD [38]. Furthermore, the bilateral R2* in quantitative MRI best distinguished MSA-P from PD, with a sensitivity of 77.8% [42];
3. DaTscan showed an earlier and more pronounced loss of dopamine transporter in the ventral putamen and anterior caudate for MSA compared to PD, but does not exclude a diagnosis of MSA [43] – some cases of MSA can have a normal DaTscan due to low degeneration of nigrostriatal dopaminergic transporters.

The more recently practiced neuroimaging techniques show a promising approach to try and differentiate MSA-P from PD, since some of these demonstrate reliable results and are more consistent than those presented for the differential diagnosis of PSP, although, these still need improvement.

## 3.3. Vascular Parkinsonism

As mentioned before, many other syndromes can mimic PD, especially at an early stage, and any of those could be taken into consideration during this work – however, one subject from the collected data presents vascular parkinsonism, so it's of full interest to, at least, briefly cover this parkinsonian syndrome and give insight into some of its aspects.

The hallmark for vascular parkinsonism (VP) consists of vascular changes in the brain, which may be ischemic or haemorrhagic. These can occur in the basal ganglia, subcortical white matter and thalamus, along with other structures. Clinical features of this syndrome include rigidity, short stepped gait, cognitive impairment and pseudobulbar palsy, but the prominent manifestation of this disorder is lower body parkinsonism, which is characterized by slow, insecure gait. Contrarily to PD but similarly to the other already described atypical parkinsonisms, cases of vascular parkinsonism show slight to no response to dopaminergic therapy, but still share many motor features with PD [44].

Neuroimaging techniques provide support for the diagnosis of VP trough MRI and DaTscan. A DaTscan of the VP brain show increased uptake of dopamine markers when

compared to PD, as their dopaminergic pathway is intact. Although, if ischemic damage is present within the striatum, the uptake is reduced. Pooled sensitivity and specificity for diagnosis of VP versus PD using DaTscan could be as high as 85% and 80%, respectively [45].

### 3.4. The relevance of a differential diagnosis

After a brief overview of the most common atypical parkinsonian syndromes, it's important to clarify the significance of a differential diagnosis between Parkinson's disease and its atypical forms. Considering all the above mentioned, it's clear that these syndromes share many clinical features, not only of motor nature but neuropathological, with many cases experiencing cognitive impairments during life, and deteriorating motor complications that worsen as the disease progresses. However, these syndromes are not equal, individually differing from one another and having different treatments and prognostics. Unfortunately, the clinical features that make a more precise differential diagnostic possible only appear in later stages, increasing the time period before a correct diagnosis is made and reducing the likelihood of getting the best treatment results, since these are usually only achieved when early applied. Therefore, these syndromes should be individually tackled for what they are as soon as possible so that the patient can experience the best possible outcome for their condition, and not be incorrectly treated for a condition they don't have, which sometimes might even induce unwanted drug therapy side effects.

# 4. Movement analysis based on Inertial sensors

## 4.1. Overview on inertial sensors

Inertial sensors, also called Inertial Measurement Units (IMU), are sensors capable of measuring their own movement, thus measuring the movement of the object they are attached to. An IMU is classically composed of three individual types of sensors: accelerometer, gyroscope and magnetometer. An accelerometer measures the acceleration of a body along an axis by determining the inertia of a mass when it experiences an external force. Depending on the working principle, accelerometers can be capacitive, piezoelectric or piezoresistive, and in theory, they convert a mechanical force into an electric signal. Because an accelerometer can only measure acceleration relative to a fixed axis, IMUs usually combine three accelerometers in order to measure acceleration in three orthogonal axes. Combined with accelerometers, IMUs also incorporate gyroscopes which are responsible for measuring angular velocity when external torque is applied, based on the Coriolis force, which is an apparent force proportional to the angular rate of rotation of a rotating reference frame [46]. These are usually mounted in the same 3D arrangement as accelerometers, in order to measure angular velocity in three orthogonal axes. Finally, IMUs also feature a 3D magnetometer which measures the earth magnetic field, helping with sensor orientation.

On most applications, however, IMUs are generally manufactured as a microelectromechanical system (MEMS), which is a type of technology for manufacturing microscopic devices with moving parts. These devices are therefore small, light-weight and easily adaptable to most applications.

## 4.2. Gait and postural analysis

Human gait corresponds to the physiological way of locomotion [47]. It consists of a cyclic, coordinated movement of the body segments and comprises two distinct phases: swing and stance. The stance phase begins with the initial contact when the heel touches the ground, also called heel strike. As the body moves forward, the load response begins, followed by the midstance as the contralateral leg moves forward in relation to the reference leg. The terminal stance follows as the heel leaves the ground (heel off) and the stance phase ends with the pre-swing, with the toes pushing down and giving momentum for the swing phase. This phase begins with the initial swing (toe off), midswing as the reference leg passes the contralateral leg, and finally the terminal swing, ending the gait cycle as the heel touches the ground again. During normal human locomotion, this cycle is repeated over and over again. It's important to understand these events because they condition the relevant gait parameters that inertial sensors are afterwards able to quantify. For instance one gait step (measured either in time or length) goes between the heel strike of one leg and the heel strike of the contralateral leg; step width refers to the mediolateral distance between the two feet; one stride comprises a whole gait cycle, or two sequential steps; double support corresponds to the moment when both feet are touching the ground (one in initial contact and the other in pre-swing); single support corresponds to the time between the reference pre-swing and contralateral initial contact, which in turn represents the same as the contralateral swing phase (see figure 4 for further reference).

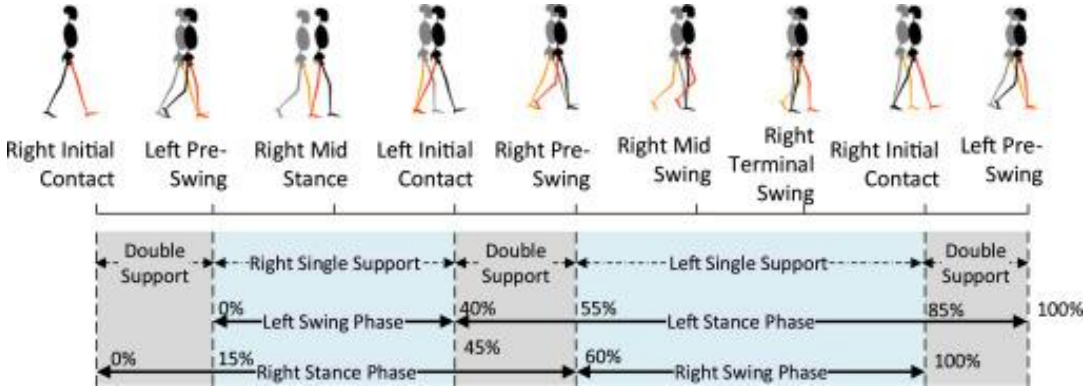


**Figure 4** - Gaits' phases (stance and swing) and their respective stages. Adapted from Papavasileiou et al. (2017). Real-time Data-driven Gait Phase Detection using Ground Contact Force Measurements: Algorithms, Platform Design and Performance.

When all these events are measured on both sides along with the movements (rotation, adduction, flexion and extension) and angles performed by the joints engaged during gait (hip, knee and ankle), an array of features can be extracted from gait and used to quantify it. This is rather helpful when one wants to compare standard and abnormal gait characteristics, like the ones seen in patients with neurological disorders (such as PD and the already mentioned atypical forms of parkinsonism). Furthermore, when the aforementioned sensors are taken into consideration, it's possible to position them on strategical points within the human body to create a 3D network of data that, when integrated with complex feature extraction algorithms, allows for the extraction of a series of spatio-temporal kinematic parameters.

Many studies have already been conducted using inertial sensors to assess gait in PD patients. To name a few, Schlachetzk and colleagues reported that wearable sensor-based gait analysis can reach clinical applicability and provided high biomechanical resolution for gait impairment in a 190 PD patient cohort [48]; spatio-temporal kinematic parameters such as increased double support time, reduced gait speed and step/stride length and decreased gait symmetry have been correlated with PD [49]; Curtze and colleagues studied levodopa and its' effects using inertial sensors on a 104 subject cohort and was able to assess postural stability and gait dynamics [50]. Furthermore, sensor number and positioning have been reviewed by Brognara and his group and found that the best sensor arrangement and feature combination for assessment of PD is not yet clear, with high variability between studies [5]. Last but not least, the number of studies that evaluate gait in patients with atypical parkinsonian syndromes and compare them to PD/healthy control cohorts are very limited, although, Raccagni and colleagues conducted a study with 25 PD patients and 25 atypicals (12 PSP and 13 MSA) and found that the latter group showed reduced gait speed and stride length compared to both PD and control cohorts [51]. Anyway, this study was performed using only laterally mounted inertial sensors on both feet, which highly reduces the amount of spatio-temporal kinematic parameters that can be measured.

Considering the abovementioned, it's safe to say that established sensor arrangement and standard protocols for data acquisition of gaits' kinematic parameters for both PD and its atypical forms are lacking; therefore, from a technological, engineering and reproduceable point of view it is paramount to develop a consistent protocol that is able to collect as many

spatio-temporal features as possible, analyse and eventually reduce them to a set of significant parameters that are able to distinguish between these disorders.

### 4.3. Finger tapping analysis

Finger tapping consists of consecutively hitting the thumb and index finger together, in a fast and periodic motion. Compared to gait it's a very basic movement but one that is used in common practice as a bradykinesia test. As mentioned before, bradykinesia is a clinical feature of PD that describes slowness of movement and reduction in speed and amplitude of repetitive actions. Indeed, for the trained eye, this is a detectable feature during a finger tapping test and one that can provide helpful diagnostic clinical clues, but as all other features of PD, it can be object of subjective quantification due to expertise variability between examiners. Recently some work has been done in order to quantify bradykinesia. Ling and colleagues used infrared LEDs to assess bradykinesia during finger tap tests for PD (n=15) versus PSP (n=9) cohorts and concluded that "bradykinesia without decrement distinguishes progressive supranuclear palsy from Parkinson's disease", meaning that they saw no reduction in average finger separation amplitude for PSP, which was notable in PD cases (p=0.002) [35]. Jovičić and colleagues studied the same events in 13 PD patients, 15 PSP and 14 MSA using inertial sensors and, similarly to the previous mentioned study, found minimal progressive reduction in amplitude during finger taps for the PSP group, but significant reduction for the PD and MSA groups (p=0.001 and p=0.003, respectively), which led them to the same conclusions. Recently, the same group also developed an expert system for quantification of bradykinesia based on inertial sensors and achieved an overall accuracy of 83% when testing for finger tapping and based on the reference scores provided by two neurologists [52]. It is therefore safe to say that finger tapping represents a solid test for assessment of bradykinesia, but automated analysis techniques for feature extraction are still required for reliable quantification.

## 5. Machine Learning

Machine learning (ML) is a field within computer science which is able to build an algorithm (or model) from input data and predict an output, while updating its model as more data becomes available. ML algorithms are usually classified into either supervised and unsupervised. In supervised learning, labelled data is used in order to predict the classification of other unlabelled data. Algorithms based on supervised learning are linear and logistic regression, k-nearest neighbours, classification trees, support vector machine, etc. For unsupervised learning, on the other hand, data fed into the model is not labelled or classified, therefore allowing the algorithm to discover structure and patterns within the data. Common unsupervised algorithms are clustering (k-means, hierarchical), principal component analysis, etc. The machine learning approach of this work comes from an exploratory standpoint, and not from a classification performance point of view. It's beyond the scope of this work to investigate the most optimal algorithm and its adjustments, let alone compare different classification algorithms. That said, it at least makes sense to cover the adopted algorithm for this work, which was random forest (explanation at materials and methods for why it was chosen). Sampling, feature selection and scoring methodologies will also be briefly covered.

Random forests consist of a large number of decision trees (therefore, supervised learning) that operate as an ensemble [53]. To classify a new data entry, each individual decision tree makes a prediction and the random forest collects all predictions, choosing the most voted one and making it the model's prediction. It's a powerful machine learning tool because it enables a large number of weakly correlated or uncorrelated models to form a strong classifier and is able to handle large sets of features with a reduced sample size [54]. This is a key characteristic because the data used for this work has far greater number of features compared to instances.

An important element of machine learning is feature selection, which is the process of selecting a subset of features that will relevantly help the model's construction. Prior work developed during this master's degree for *Aprendizagem Automática* using a similar dataset revealed that the best performing feature selection technique was through information gain ratio when working with decision trees and random forests. Information gain ratio is the ratio between the expected amount of information that a feature can provide about a class and the features' intrinsic information. It's quite effective in decision trees because it reduces bias towards multivalued features. Another important aspect to discuss is sampling. In this case, k-fold cross validation was used, which comprises of a resampling procedure used to evaluate the skill of an algorithm to classify new, unseen data. The k usually takes the form of a number, such as 10, making it 10-fold cross validation. This nomenclature means that the dataset is split into k groups, where one group is kept as a test set and the remaining groups as training sets. Then, the model is fitted on the training set and evaluated on the test set. This procedure loops for k-1 folds until all sets have been used as both training and test. For instance, in a dataset with 100 data entries, 10-fold cross validation will split the data into 10 groups of 10 data entries each, with one group acting as a test set and the remaining 9 as training sets, looping until all data groups act as both training as testing. Using 10-fold cross validation is a safe approach because it has been empirically shown to reduce both bias and variance [55].

Finally, an overview on the different ways one can evaluate the performance of a machine learning model. First, confusion matrix. The confusion matrix (table 3) is a table that

allows one to visually understand the performance of a model by checking how many predictions were correct and incorrect. Correct predictions correspond to the true negatives and true positives, whereas incorrect predictions correspond to the false negatives and false positives. Using this works example: let's say a model can only predict a subject as either 'control' (negative) or 'ill' (positive):

- True negatives are the subjects that are actual controls and are predicted as controls;
- True positives are the subjects that are actually ill and are predicted as ill;
- False negatives are the subjects that are actually ill but are predicted as controls;
- False positives are the subjects that are actual controls but are predicted as ill.

**Table 3** - Example of a confusion matrix

| | | **Predicted** | |
|---|---|---|---|
| | | Control | Ill |
| **Actual** | Control | True negative | False positive |
| | Ill | False negative | True positive |

From this table, some scores can be computed in order to quantify the performance of a model: classification accuracy, F1, precision and recall.

$$Classification\ accuracy = \frac{True\ positives + True\ negatives}{Total\ of\ subjects}$$

$$Precision = \frac{True\ positives}{True\ positives + False\ positives}$$

$$Recall = \frac{True\ positives}{True\ positives + False\ negatives}$$

$$F1 = 2 * \frac{Recall * Precision}{Recall + Precision}$$

# 6. Materials and Methods

## 6.1. Participants

All participants included in this study were recruited at Hospital Egas Moniz, Centro Hospitalar de Lisboa Ocidental (CHLO). Patients with PD or atypical parkinsonism were sequentially recruited from the outpatient clinic in routine appointments. Patients were evaluated by one element of the research team (a neurology resident or neurologist trained in movement disorders). Participants with PD and atypical parkinsonism were recruited independently of disease duration and/or characteristics. The only exclusion criteria consisting of being incapable of performing the required tasks (i.e. incapable of walking without aid, wheelchair bound). Subjects without any evidence of motor disease accompanying patients observed in the Neurology outpatient clinic were invited to participate as control subjects. Controls consisted of subjects that had no known diagnosis of a neurological disorders (headaches were not excluded) and did not report any sign and symptom suggesting the presence of motor dysfunction. Controls were age matched for PD patients. Personal and clinical data collected from the subjects consisted of age, gender, disease duration and Levodopa Equivalent Daily Dose (LEDD – represents the amount of levodopa taken daily as a contribution of each parkinsonian drug. Computed using the Levodopa Equivalent Dose Calculator available at www.parkinsonsmeasurement.org [56], [57]) (both not applicable for the control group), and motor MDS-UPDRS. Participants were divided into three, age-gender matched groups (table 4): a Parkinson's disease group (n=32, mean age 69,7 ± 11,3), atypical parkinsonism group (n=11, mean age 72,9 ± 6,1) and a healthy control (HC) group (n=33, mean age 68,0 ± 12,6).

An informed written consent approved by the Ethics Committee for Health of CHLO was presented and signed by every participant, thoroughly clarifying the objectives, conditions, risks and benefits of the study. For each participant, the informed consent was stored, along with the personal and clinical data.

**Table 4** - Clinical and demographic data for PD (n=32), HC (n=33) and atypical parkinsonism (9 PSP, 1 MSA, 1 vascular parkinsonism; n=11) groups.

| Parameters | Healthy Controls | Parkinson's Disease | Atypical Parkinsonism |
|---|---|---|---|
| **Nº of subjects** | 33 | 32 | 11<br>(9 PSP, 1 MSA, 1 VP) |
| **Age, years** | 68,0 ± 12,6 | 69,7 ± 11,3 | 72,9 ± 6,1 |
| **Male/Female** | 14/19 | 15/17 | 8/3 |
| **Disease duration, years** | - | 4,8 ± 4,3 | 4,9 ± 2,0 |
| **LED, mg/day** | - | 395,2 ± 302,0 | 339,1 ± 209,0 |
| **Motor UPDRS** | 2,5 ± 3,4 | 29,0 ± 13,5 | 31,0 ± 12,3 |

## 6.2. Assessment Protocol

The assessment protocol included two tests that each participant had to perform. The first one consisted of a finger tapping test, in which the participants were asked to tap (open and close, together) their thumb and index finger consecutively for thirty seconds, as fast and wide as possible. Participants were free to perform this test as good as his/her physical

condition allowed, with the only prerequisite being that the arm must be stable as much as possible during the test, and only the fingers are allowed to move. The second test consisted of gait and postural stability analysis. For assessment of postural stability, the participants were asked to stand still with both their feet apart and together, each one for thirty seconds, while trying to maintain as much of a stable position as possible. Then, for gait assessment, participants were asked to walk in a straight line back and forth three consecutive times in a 10m long predetermined course, without any external help. During both finger tapping and gait/stability tests, kinematic data was collected using suitable inertial sensors that will be discussed in the Hardware section.

## 6.3. Hardware

### 6.3.1. HARP - WEAR

The hardware used to evaluate finger taps was developed by the Champalimaud Foundation Hardware Platform (HARP), a platform focused on developing electronic and mechanical tools for scientific research support. HARP provides devices for kinematic data acquisition within the WEAR family of devices. The list of material used goes as follows:

- Two WEAR wireless sensor devices v2.1
- Two WEAR basestations v1.2
- One WEAR charger dock v2.1
- One clock synchronizer v1.0
- Two 3.5mm stereo jack connectors
- Three USB type B-mini cables

The WEAR sensors (figure 5.A) have a configurable sampling rate up to 200Hz and connect wirelessly with the basestations (figure 5.B), that in turn connect with the computer via type B-mini USB's. At the same time, both basestations are connected to a clock synchronizer (figure 5.C) via 3.5mm stereo jacks, allowing the collected data from both sensors to be temporally aligned. The 45 mAh sensor batteries are charged in the WEAR charger dock, which can charge up to 4 sensors at a time (figure 6). Finally, attend to figure 7 for a visual and schematic representation of the abovementioned assembly.

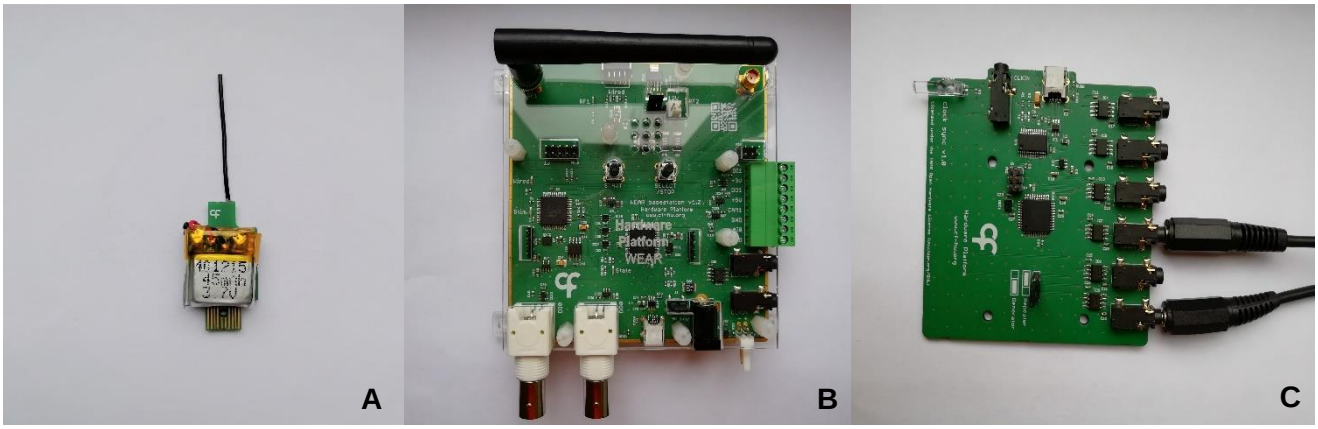


**Figure 5** - A) WEAR wireless sensor, B) WEAR basestation, C) Clock synchronizer

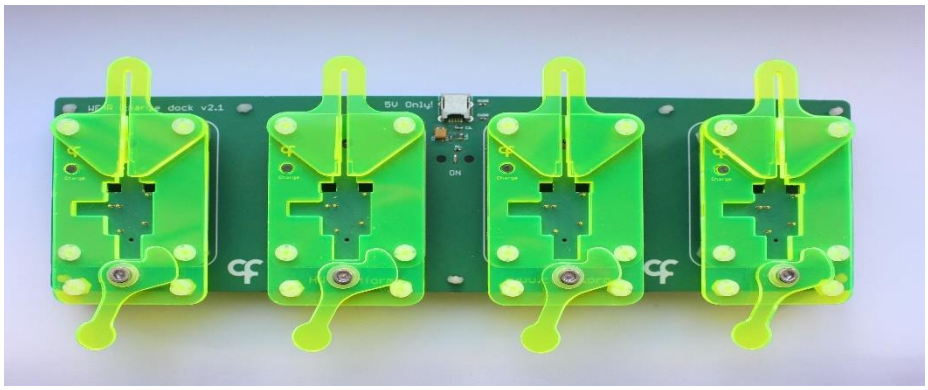

**Figure 6** - WEAR charging dock

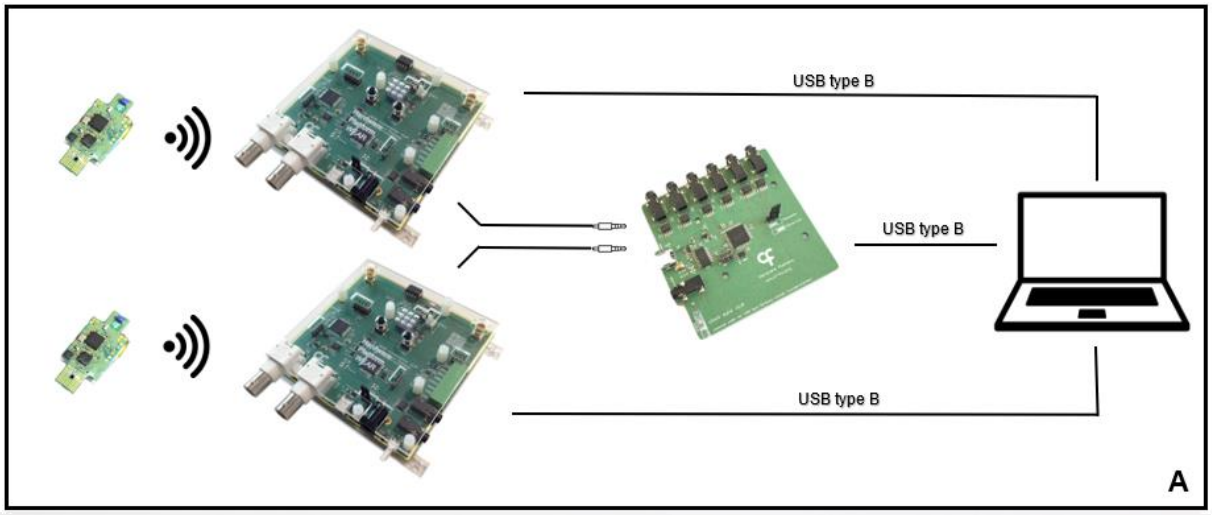


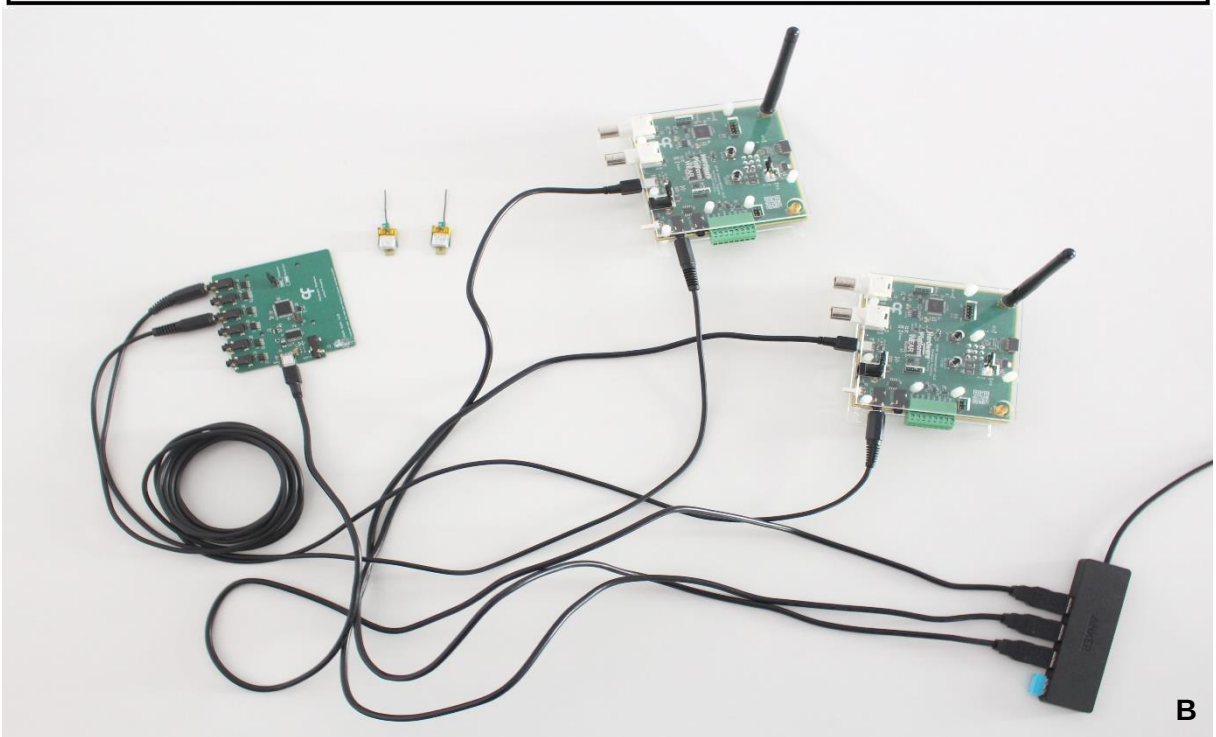


**Figure 7** – A) WEAR sensor and basestation schematic assembly; B) WEAR sensor and basestation setup visual representation

### 6.3.2. Xsens – MTw Awinda

The MTw Awinda from Xsens is a 3D human wireless motion tracker that utilizes a body area network of wearable sensors for accurate, unobtrusive motion tracking. Depending on the application these sensors can be used in a wide range of configurations, with an internal sampling rate of 1000Hz, data synchronization time of 10 µs, up to 6 hours of battery life during continuous use and easily placement with the help of Velcro straps. The material used and number of sensors depends on the desired configuration, but for this case in particular, it goes as follows:

- Seven MTw Awinda Wireless 3DOF motion tracker
- One Awinda docking station
- Seven Velcro straps (various sizes)
- One USB type B cable

The setup is similar to the abovementioned, but fairly easier to implement. In this case, the sensors (figure 8.A) are individually turned on, and wirelessly synchronize with the docking station (figure 8.B), which in turn connects with the computer via a USB type B cable. The sensors battery is charged via the docking station, which can charge up to 6 sensors at a time. Finally, refer to figure 9 for a schematic representation of this assembly.

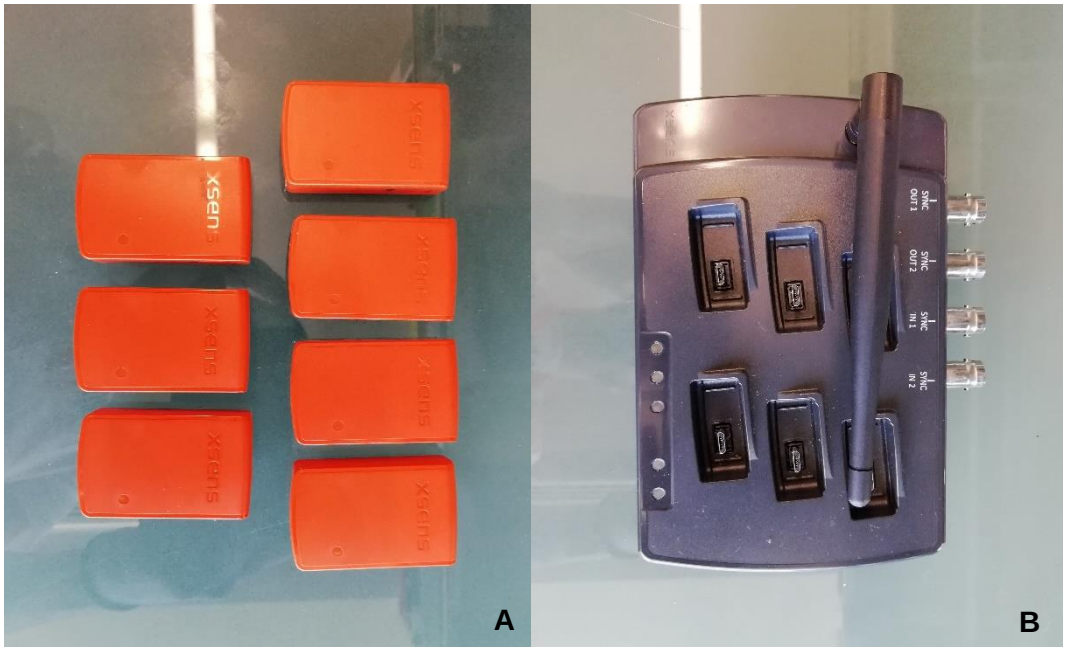


**Figure 8** - A) MTw Awinda Wireless 3DOF motion trackers; B) MTw Awinda docking station

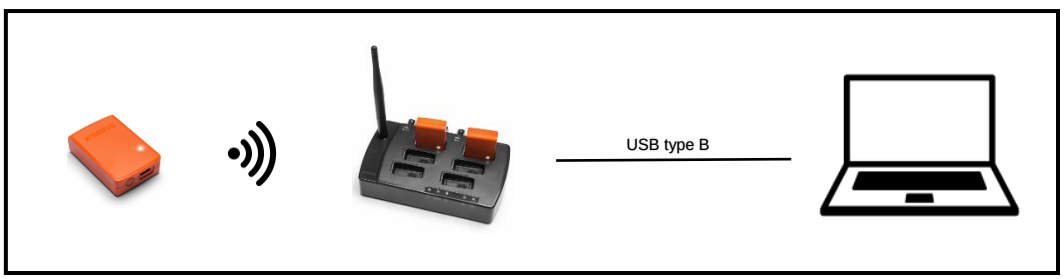


**Figure 9** - Schematic representation of the MTw Awinda motion tracker setup

## 6.4. Data acquisition and processing

### 6.4.1. Finger tapping

During the neurology appointment and after giving consent, participants were asked to perform the required tests for the study. Finger tapping was assessed first, and for this, the two sensors were positioned on top of the thumb and index finger of their most affected side using medical tape, with the battery pointing upwards and antenna pointing outwards, like in figure 10 (in this picture clear tape was used for demonstration purposes). Participants were given the freedom to either keep their arm slightly raised or to rest the elbow on a surface, in case they were not able to maintain a stable position. A digital clock was then set to 30 seconds and when both participant and operator were ready, the test would start after hitting the START button on both basestations and the Bonsai software. This software was not only responsible for recording the collected data but also allowed the operator to keep track on the behaviour of the sensors and to look for any sensor malfunction during the test, since it displays real-time readings of all three axis for the accelerometer, gyroscope and magnetometer (figure 11). This was particularly important in case the sensors had their battery drained, since the software would show no readings for the sensor in question.

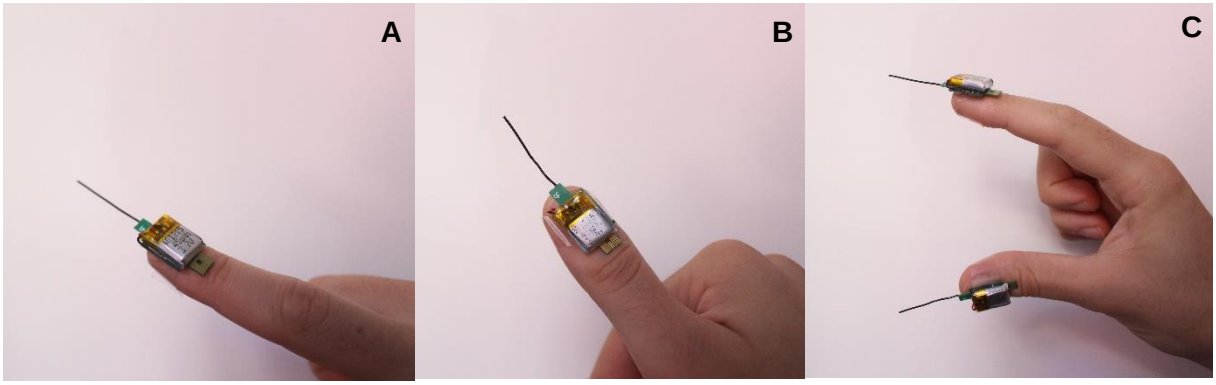


**Figure 10** - Sensor positioning in the index finger (A), thumb (B), and both (C)

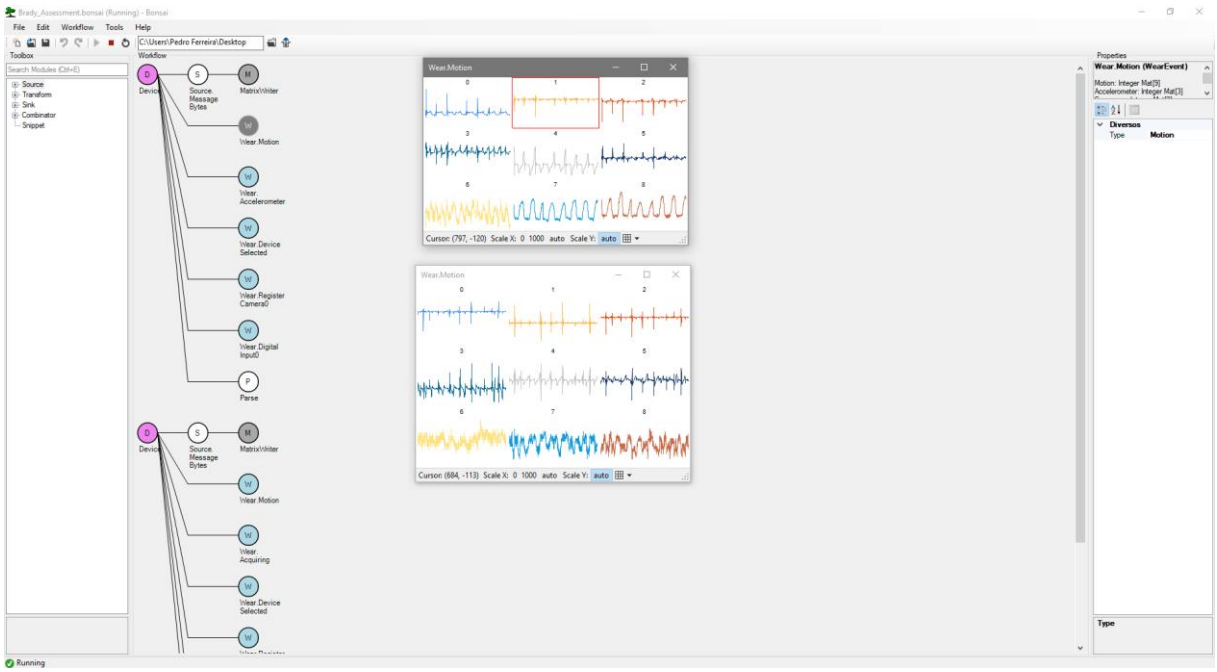

**Figure 11** - Bonsai software displaying real time readings of all axis of accelerometer, gyroscope and magnetometer

The test ends after 30 seconds when hitting the STOP button on the Bonsai software and the sensors are carefully removed from the participants' fingers.

### 6.4.2. Gait and postural stability

After testing the finger tapping, participants were asked to stand up and seven MTw Awinda inertial sensors were placed using Velcro straps in the following locations: midline of the back, left and right thigh, left and right ankle and back of the left and right foot (figure 12). When turned on, a red blinking LED light will appear, which must be facing downwards in the case of the sensor in the back; for the remaining sensors, this light must be facing backwards. The sensors were then calibrated, and two tests were performed: for the first one, participants were asked to stand still for 30 seconds with their feet apart and 30 more seconds with their feet together, for assessment of postural stability. Afterwards, subjects were asked to walk back and forth three times in a 10m long, unobstructed corridor, making a total of 60 meters. Participants were given instructions to walk in a straight line as best as possible, without help and without stopping. The start and end points of the course were marked on the floor with a white strip. During the walking period, the collected data was being transferred to the computer via the docking station through the Link software. This software, along with the pattern recognition software used to process the raw data acquired from gait and postural stability tests, was made available by Kinetikos.

**Figure 12** - Sensor positioning for gait and postural stability tests. 1. Midline of the back, 2. Right thigh, 3. Left thigh, 4. Right ankle, 5. Left Ankle, 6. Right foot, 7. Left foot

After acquisition, a set of raw data files was generated for each participant, that were later uploaded to the Kinetikos Platform where they're processed. This platform takes care of the signal processing and data modelling, from which an array of spatio-temporal parameters is then retrieved, up to 103 in total. These parameters can be divided into three groups: traditional gait parameters, angular parameters and nonlinear parameters. Traditional gait parameters include the typically assessed gait metrics which can be seen below (table 5). In total, 33 traditional gait parameters were acquired. Some of these parameters, like speed, can be assessed on both sides independently (right/left) or as an average of both.

**Table 5** - Acquired traditional spatio-temporal gait parameters and respective measurement units.

| **Gait metrics** | | **Measurement units** | | | | |
|---|---|---|---|---|---|---|
| | | [m/s] | [steps/min] | Time [s] | Length [m] | Percentage of cycle [%] |
| **Speed** | | X | | | | |
| **Speed** | Right / Left | X | | | | |
| **Cadence** | | | X | | | |
| **Step time** | Right / Left | | | X | | |
| **Step length** | | | | | X | |
| **Stride time** | | | | X | | |
| **Stride time** | Right / Left | | | X | | |
| **Stride length** | | | | | X | |
| **Step width** | | | | | X | |
| **Step width** | Right / Left | | | | X | |
| **Stance fraction** | | | | | | X |
| **Stance time** | | | | X | | |
| **Swing fraction** | | | | | | X |
| **Swing time** | | | | X | | |
| **Double support** | | | | | | X |
| **Double support** | | | | | | X |
| **Double support time** | Right / Left | | | X | | |
| **Double support time** | | | | X | | |
| **Single support** | Right / Left | | | | | X |
| **Single support time** | | | | X | | |

Angular parameters are usually described as range of motion (RoM) features. RoM stands for the difference between the maximum and minimum angles achieved in the sagittal plane between two adjacent articular segments within one gait cycle. RoMs assessed in this work include the pelvic, hip, knee and ankle joints, associated with rotation, adduction and extension movements, making a total of 44 parameters. For instance, the 'hip flexion rom R' parameter refers to the range of motion performed by the right hip during flexion motion, while the 'ankle angle rom R' refers to the range of motion angle performed by the right ankle joint. All the speed and angular parameters acquired in this work can be consulted in the table 6, with the respective measuring units.

**Table 6** - Acquired speed and angular gait parameters and respective measurement units.

| Gait metrics | Measurement Units | |
|---|---|---|
| | Degrees [°] | [cm/s] |
| **Pelvis list. RoM** | X | |
| **Hip flexion RoM** | X | |
| **Hip adduction RoM** | X | |
| **Hip rotation RoM** | X | |
| **Knee angle RoM** | X | |
| **Ankle angle RoM** | X | |
| **Pelvis list. mean velocity** | | X |
| **Hip flexion mean velocity** | | X |
| **Hip adduction mean velocity** | | X |
| **Hip rotation mean velocity** | | X |
| **Knee angle mean velocity** | | X |
| **Ankle angle mean velocity** | | X |

The third group of gait related parameters consist of those non-linear. For instance, the harmonic ratios (HR) were obtained from the trunk acceleration (based on sensor 1), through the analysis of variation of frequency amplitude and giving insight into balance during gait. These were measured on the anterior-posterior (AP), vertical (Vert.) and medio-lateral (ML) planes. Another set of measured non-linear parameters consist of the displacement of center of mass along the aforementioned planes, that is: displacement of center of mass along the anterior-posterior plane (CoM rms AP), vertical plane (CoM rms Vert.) and medio-lateral plane (CoM rms ML). Being non-linear, these parameters have no measurement units.

From a clinical point of view, it makes little sense to compare right/left between groups because of the high variability associated. For instance, one patient may display a more affected right side, compared to another patient with a more affected left side. Because of this it was advised to create, for each parameter measured on both sides, another one that considers the worst affected side of each patient. This ‘worst-side’ label was given to every participant by a neurologist, based on the motor UPDRS scale of each patient.

Following this trend, all parameters measured on both sides (those on tables 5 and 6) have a respective worst-side variable that will be used to compare kinematic parameters between groups. That said, the individual right/left parameters will not be considered on the final analysis and will only contribute to compute the correspondent worst-side variable.

Asymmetry was also computed for all the right/left variables. Unlike the worst-side approach, asymmetry refers to the difference between one side and the other, which is particularly substantial when trying to understand how much the patients motor performance varies right/left. Again, for all parameters measured right/left, asymmetry was computed as the modulus of the difference between the left side and the right side, accounting for asymmetries that would otherwise be negative.

Finally, considering all the original variables retrieved from the Kinetikos platform and those post-processed (worst-side and asymmetry), the total count is: 43 traditional gait parameters, 66 angular parameters, 18 non-linear parameters and 35 asymmetric parameters, making a total of 162 spatio-temporal gait parameters.

### 6.5. Statistical analysis and machine learning

Statistically different spatio-temporal kinematic parameters between groups were detected using the Student's t-test, with the null hypothesis stating that there is no statistical significance between the means of each parameter for each group. The alternative hypothesis states that there is statistical significance between the means of each parameter for each group. Significance was considered with $p < 0.05$. Statistical association between the kinematic parameters and clinical data was assessed using the Pearson's correlation coefficient (r): $r = 0$ meaning there was no statistical correlation; $r = 1$ meaning there was perfect positive statistical correlation; $r = -1$ meaning there was perfect negative statistical correlation. Student's t-test was computed using Python's SciPy statistical functions package (scipy.stats) version 1.2.1. Pearson's correlation was computed using Python Pandas package version 0.24.2.

Machine learning was done through the Orange machine learning toolkit version 3.20.1. Feature selection was done through information gain ratio at a fixed 6 best ranked features. For reasons mentioned before, sampling was performed using 10-fold cross validation. On a previous work developed during this master's degree for the *Aprendizagem Automática* subject, random forest was the best scoring algorithm when testing for the same kind of data, and thus was the one considered for this work. The random forest properties go as follows: number of trees = 14; number of attributes considered at each split = 3; fixed seed for random generator = On and 0; do not split subsets smaller than: 5. For ease of understanding, classification accuracy (CA) will be the score used to evaluate model performance, but all other scores will also be presented.

# 7. Results

This chapter will be separated into four sections: the first section will account for the statistical analysis of the aforementioned gait parameters for two distinct comparisons – Control vs Ill (PD + Atypical) and PD vs Atypical, with the results individually analysed for spatio-temporal variables, velocity and angular variables, non-linear variables and asymmetry variables; the second section accounts for the correlation between the collected kinematic parameters and the patients clinical data such as disease duration and motor-UPDRS; the third section will consist of an exploratory machine learning approach to create a classifier that is able to distinguish between Control/Ill and PD/Atypical, and assess its performance; finally, the fourth section gives insight into the finger tapping analysis.

The tables presented in section I and II contain, as mentioned before, only the meaningful kinematic variables, which means that no L/R variables will be analysed, only the respective worst sides, asymmetries, and those variables which are not analysed bilaterally (which is the case of speed – it can be analysed on each side or as a whole). Since not all parameters are statistically significant, these who are will be identified in bold and underlined.

## 7.1. Section I - Analysis of gait parameters

### 7.1.1. Controls vs Ill (PD + atypical)

**Table 7** – Spatio-temporal parameters for controls (n=32) vs PD + atypical group (n=39)

| | Control | Ill (PD + atypical) | p-value |
|---|---|---|---|
| **Cadence [steps/min]** | 109.420 ± 12.519 | 100.566 ± 13.432 | **0.006** |
| **Step time (worst side) [s]** | 0.557 ± 0.064 | 0.608 ± 0.080 | **0.005** |
| **Step Length (worst side) [m}** | 0.512 ± 0.086 | 0.442 ± 0.100 | **0.003** |
| **Step width [m]** | 0.190 ± 0.046 | 0.205 ± 0.084 | 0.373 |
| **Step width (worst side) [m]** | 0.189 ± 0.057 | 0.203 ± 0.084 | 0.430 |
| **Stride time [s]** | 1.109 ± 0.129 | 1.253 ± 0.345 | **0.031** |
| **Stride time (worst side) [s]** | 1.109 ± 0.129 | 1.203 ± 0.160 | **0.010** |
| **Stride length [m]** | 1.097 ± 0.140 | 0.920 ± 0.181 | **< 0.001** |
| **Stance fraction (worst side) [%]** | 68.196 ± 1.709 | 69.581 ± 2.654 | **0.014** |
| **Stance time (worst side) [s]** | 0.757 ± 0.101 | 0.875 ± 0.261 | **0.020** |
| **Swing fraction (worst side) [%]** | 31.804 ± 1.709 | 30.419 ± 2.654 | **0.014** |
| **Swing time (worst side) [s]** | 0.351 ± 0.035 | 0.378 ± 0.091 | 0.119 |
| **Double support [%]** | 36.355 ± 3.253 | 39.827 ± 5.685 | **0.003** |
| **Double support (worst side) [%]** | 18.467 ± 1.789 | 20.253 ± 3.051 | **0.005** |
| **Double support time [s]** | 0.405 ± 0.072 | 0.508 ± 0.195 | **0.007** |
| **Double support time (worst side) [s]** | 0.205 ± 0.037 | 0.257 ± 0.095 | **0.006** |
| **Single support (worst side) [%]** | 31.841 ± 2.084 | 29.754 ± 3.700 | **0.007** |
| **Single support time (worst side) [s]** | 0.352 ± 0.040 | 0.367 ± 0.090 | 0.387 |

Spatio-temporal kinematic parameters (table 7) showed that cadence was higher for the control group, and the step related variables of time and length were lowered for the parkinsonian group. Stride time was also higher for this group, with stride length being consequently lower compared to controls. Stance phase was longer in the parkinsonian group, but oppositely, swing was higher for controls. All variables related to double support were significantly increased in the parkinsonian group, but with lower single support fraction of gait compared to controls. Spatio-temporal kinematic variables of step width, swing time (worst side) and single support time (worst side) showed no statistical significance differentiating between both groups.

**Table 8** – Speed and angular parameters for controls (n=32) vs PD + atypical group (n=39)

| | Control | III (PD + atypical) | p-value |
|---|---|---|---|
| **Speed [m/s]** | 0.996 ± 0.190 | 0.773 ± 0.202 | **<0.001** |
| **Speed (worst side) [m/s]** | 0.941 ± 0.218 | 0.743 ± 0.205 | **<0.001** |
| **Pelvis list. rom (worst side) [º]** | 5.072 ± 2.020 | 4.905 ± 1.960 | 0.729 |
| **Hip flexion rom (worst side) [º]** | 38.282 ± 5.943 | 33.587 ± 6.467 | **0.003** |
| **Hip adduction rom (worst side) [º]** | 11.740 ± 3.984 | 12.414 ± 5.971 | 0.591 |
| **Hip rotation rom (worst side) [º]** | 13.207 ± 2.984 | 11.739 ± 3.286 | 0.057 |
| **Knee angle rom (worst side) [º]** | 50.726 ± 8.904 | 45.392 ± 9.211 | **0.017** |
| **Ankle angle rom (worst side) [º]** | 29.555 ± 6.830 | 28.949 ± 7.481 | 0.728 |
| **Pelvis list. mean vel. (worst side) [cm/s]** | 11.170 ± 6.750 | 9.715 ± 4.828 | 0.297 |
| **Hip flexion mean vel. (worst side) [cm/s]** | 67.900 ± 14.974 | 55.180 ± 12.814 | **<0.001** |
| **Hip adduction mean vel. (worst side) [cm/s]** | 22.927 ± 8.266 | 21.682 ± 8.819 | 0.548 |
| **Hip rotation mean vel. (worst side) [cm/s]** | 27.022 ± 6.359 | 23.473 ± 7.317 | **0.036** |
| **Knee angle mean vel. (worst side) [cm/s]** | 106.610 ± 26.384 | 85.715 ± 23.158 | **0.001** |
| **Ankle angle mean vel. (worst side) [cm/s]** | 66.370 ± 14.703 | 56.065 ± 14.877 | **0.005** |

Speed and angular parameters (table 8) analysis revealed that gait speed was considerably decreased in the parkinsonian group. For the angular parameters, those which displayed statistical significance were hip flexion and rotation and knee angle range of motion, which were all lowered compared to controls; furthermore, hip flexion and rotation and knee and ankle angles mean velocity were also lowered in the PD/atypical group, with the remaining parameters showing no significance.

**Table 9** – Non-linear kinematic parameters for controls (n=32) vs PD + atypical group (n=39)

| | Control | Ill (PD + atypical) | p-value |
|---|---|---|---|
| **Entropy AP** | 0.489 ± 0.399 | 0.839 ± 0.492 | **0.002** |
| **Entropy ML** | 1.591 ± 0.332 | 1.725 ± 0.247 | 0.058 |
| **Entropy Vert.** | 1.421 ± 0.442 | 1.540 ± 0.447 | 0.270 |
| **HR AP** | 1.705 ± 0.942 | 1.422 ± 0.759 | 0.170 |
| **HR Vert.** | 1.962 ± 1.398 | 1.273 ± 0.767 | **0.011** |
| **HR ML** | 3.585 ± 2.063 | 3.141 ± 1.972 | 0.363 |
| **CoM rms AP** | 0.019 ± 0.010 | 0.022 ± 0.011 | 0.352 |
| **CoM rms Vert.** | 0.010 ± 0.002 | 0.010 ± 0.000 | 0.265 |
| **CoM rms ML** | 0.011 ± 0.003 | 0.012 ± 0.007 | 0.552 |
| **Ampl. harm x** | 0.939 ± 0.315 | 0.945 ± 0.267 | 0.930 |
| **Ampl harm y** | 1.021 ± 0.262 | 0.933 ± 0.305 | 0.209 |
| **Ampl harm z** | 1.078 ± 0.349 | 1.015 ± 0.303 | 0.420 |
| **Width harm x** | 0.703 ± 0.206 | 0.746 ± 0.215 | 0.397 |
| **Width harm y** | 0.672 ± 0.141 | 0.741 ± 0.201 | 0.114 |
| **Width harm z** | 0.658 ± 0.141 | 0.669 ± 0.177 | 0.765 |
| **Slope harm x** | 1.601 ± 0.670 | 1.778 ± 1.559 | 0.557 |
| **Slope harm y** | 1.772 ± 0.666 | 2.122 ± 1.970 | 0.348 |
| **Slope harm z** | 2.348 ± 1.313 | 3.277 ± 2.884 | 0.102 |

Only two non-linear gait related parameters (table 9) were significant enough in differentiating between controls and the parkinsonian group, which were entropy AP (double in the parkinsonian group compared to controls) and the balance harmonic ratio along the vertical axis, which was higher for the control group.

**Table 10** - Asymmetry parameters for controls (n=32) vs PD + atypical group (n=39)

| | Control | Ill (PD + atypical) | p-value |
|---|---|---|---|
| **Step time asymmetry [s]** | 0.022 ± 0.020 | 0.107 ± 0.427 | 0.274 |
| **Step length asymmetry [m]** | 0.081 ± 0.066 | 0.074 ± 0.070 | 0.668 |
| **Step width asymmetry [m]** | 0.044 ± 0.036 | 0.029 ± 0.024 | **0.043** |
| **Stride time asymmetry [s]** | 0.003 ± 0.005 | 0.072 ± 0.420 | 0.366 |
| **Stance fraction asymmetry [%]** | 1.508 ± 1.390 | 2.133 ± 2.377 | 0.198 |
| **Stance time asymmetry [s]** | 0.016 ± 0.017 | 0.040 ± 0.095 | 0.169 |
| **Swing fraction asymmetry [%]** | 1.508 ± 1.390 | 2.133 ± 2.377 | 0.198 |
| **Swing time asymmetry [s]** | 0.017 ± 0.016 | 0.040 ± 0.094 | 0.193 |
| **Double support asymmetry [%]** | 1.070 ± 1.001 | 1.869 ± 2.339 | 0.080 |
| **Double support time asymmetry [s]** | 0.014 ± 0.011 | 0.022 ± 0.027 | 0.097 |

| | | | |
|---|---|---|---|
| **Single support asymmetry [%]** | 1.508 ± 1.389 | 2.134 ± 2.377 | 0.199 |
| **Single support time asymmetry [s]** | 0.017 ± 0.017 | 0.040 ± 0.094 | 0.198 |
| **Pelvis list rom asymmetry [º]** | 0.166 ± 0.115 | 0.383 ± 1.517 | 0.431 |
| **Hip flexion rom asymmetry [º]** | 0.589 ± 0.521 | 0.824 ± 1.656 | 0.450 |
| **Hip adduction rom asymmetry [º]** | 0.306 ± 0.186 | 0.468 ± 0.807 | 0.280 |
| **Hip rotation rom asymmetry [º]** | 0.570 ± 0.288 | 0.689 ± 1.840 | 0.722 |
| **knee angle rom asymmetry [º]** | 0.459 ± 0.432 | 0.736 ± 1.194 | 0.223 |
| **Ankle angle rom asymmetry [º]** | 0.341 ± 0.222 | 0.422 ± 0.328 | 0.241 |
| **Pelvis list mean vel asymmetry [cm/s]** | 0.099 ± 0.088 | 0.149 ± 0.317 | 0.398 |
| **Hip flexion mean vel asymmetry [cm/s]** | 0.676 ± 0.560 | 0.968 ± 1.957 | 0.425 |
| **Hip adduction mean vel asymmetry [cm/s]** | 0.262 ± 0.165 | 0.348 ± 0.329 | 0.189 |
| **Hip rotation mean vel asymmetry [cm/s]** | 0.517 ± 0.403 | 0.579 ± 1.111 | 0.771 |
| **Knee angle mean vel asymmetry [cm/s]** | 0.934 ± 0.844 | 1.427 ± 2.033 | 0.210 |
| **Ankle angle mean vel asymmetry [cm/s]** | 0.671 ± 0.375 | 0.831 ± 0.810 | 0.314 |
| **Speed asymmetry [m/s]** | 0.154 ± 0.126 | 0.148 ± 0.144 | 0.859 |

Finally, assessment of asymmetry (table 10) showed that, overall, these parameters were not very significant when distinguishing between the control and ill group. That said, only step width asymmetry was significantly lower for the PD and atypical group compared to controls. All the remaining parameters were non-significant ($p > 0.005$).

### 7.1.2. PD vs atypical parkinsonism

**Table 11** - Spatio-temporal kinematic parameters for PD (n=31) vs atypical group (n=8)

| | **PD** | **Atypical** | **p-value** |
|---|---|---|---|
| **Cadence [steps/min]** | 101.248 ± 12.689 | 97.924 ± 16.713 | 0.540 |
| **Step time (worst side) [s]** | 0.609 ± 0.081 | 0.605 ± 0.084 | 0.909 |
| **Step length (worst side) [m]** | 0.457 ± 0.087 | 0.381 ± 0.130 | 0.054 |
| **Step width [m]** | 0.211 ± 0.091 | 0.182 ± 0.043 | 0.394 |
| **Step width (worst side) [m]** | 0.210 ± 0.092 | 0.176 ± 0.039 | 0.314 |
| **Stride time [s]** | 1.203 ± 0.157 | 1.448 ± 0.697 | 0.073 |
| **Stride time (worst side) [s]** | 1.203 ± 0.157 | 1.204 ± 0.183 | 0.986 |
| **Stride length [m]** | 0.946 ± 0.167 | 0.819 ± 0.210 | 0.076 |
| **Stance fraction (worst side) [%]** | 69.252 ± 2.358 | 70.856 ± 3.477 | 0.129 |
| **Stance time (worst side) [s]** | 0.835 ± 0.131 | 1.031 ± 0.510 | 0.056 |
| **Swing fraction (worst side) [%]** | 30.748 ± 2.358 | 29.144 ± 3.477 | 0.129 |
| **Swing time (worst side) [s]** | 0.368 ± 0.036 | 0.416 ± 0.192 | 0.187 |
| **Double support [%]** | 39.111 ± 5.737 | 42.604 ± 4.831 | 0.123 |
| **Double support (worst side) [%]** | 19.770 ± 2.922 | 22.125 ± 2.987 | 0.050 |

| | | | |
|---|---|---|---|
| **Double support time [s]** | 0.476 ± 0.123 | 0.634 ± 0.345 | **0.039** |
| **Double support time (worst side) [s]** | 0.241 ± 0.060 | 0.321 ± 0.165 | **0.030** |
| **Single support (worst side) [%]** | 30.142 ± 3.966 | 28.251 ± 1.909 | 0.202 |
| **Single support time (worst side) [s]** | 0.359 ± 0.057 | 0.399 ± 0.169 | 0.276 |

For the assessment of PD vs atypical cohorts, analysis of spatio-temporal kinematic parameters (table 11) revealed that, for the most part, variables related to the double support phase were the only significant ones, being worth mentioning double support (worst side), double support time average of both sides and double support time (worst side), which were all increased in the parkinsonian group. The remaining traditional spatio-temporal parameters showed no significance.

**Table 12** - Speed and angular kinematic parameters for PD (n=31) vs atypical group (n=8)

| | **PD** | **Atypical** | **p-value** |
|---|---|---|---|
| **Speed [m/s]** | 0.796 ± 0.200 | 0.685 ± 0.195 | 0.168 |
| **Speed (worst side) [m/s]** | 0.773 ± 0.200 | 0.629 ± 0.196 | 0.076 |
| **Pelvis list rom (worst side) [º]** | 4.799 ± 2.138 | 5.319 ± 1.011 | 0.511 |
| **Hip flexion rom (worst side) [º]** | 34.115 ± 5.966 | 31.540 ± 8.273 | 0.322 |
| **Hip adduction rom (worst side) [º]** | 12.754 ± 6.611 | 11.095 ± 1.938 | 0.491 |
| **Hip rotation rom (worst side) [º]** | 12.029 ± 3.488 | 10.617 ± 2.161 | 0.285 |
| **Knee angle rom (worst side) [º]** | 45.999 ± 9.027 | 43.040 ± 10.169 | 0.425 |
| **Ankle angle rom (worst side) [º]** | 30.482 ± 7.189 | 23.010 ± 5.621 | **0.010** |
| **Pelvis list mean vel (worst side) [cm/s]** | 9.855 ± 5.315 | 9.170 ± 2.249 | 0.726 |
| **Hip flexion mean vel (worst side) [cm/s]** | 56.133 ± 12.453 | 51.487 ± 14.395 | 0.368 |
| **Hip adduction mean vel (worst side) [cm/s]** | 22.218 ± 9.628 | 19.603 ± 4.321 | 0.462 |
| **Hip rotation mean vel (worst side) [cm/s]** | 24.234 ± 7.850 | 20.522 ± 3.747 | 0.205 |
| **Knee angle mean vel (worst side) [cm/s]** | 87.373 ± 23.950 | 79.288 ± 19.836 | 0.386 |
| **Ankle angle mean vel (worst side) [cm/s]** | 58.979 ± 14.153 | 44.772 ± 12.635 | **0.014** |

Analysis of speed and angular kinematic parameters (table 12) showed that the ankle range of motion on the worst side was considerably reduced for the atypical group compared to PD, and so was the ankle mean velocity on the worst side. Worst-side speed was also reduced for the atypical cohort, and consequently overall speed was also lower. but both of these were not statistically significant between groups, along with the remaining parameters.

**Table 13** - Non-linear kinematic parameters for PD (n=31) vs atypical group (n=8)

| | PD | Atypical | p-value |
|---|---|---|---|
| **Entropy AP** | 0.771 ± 0.501 | 1.103 ± 0.377 | 0.090 |
| **Entropy ML** | 1.709 ± 0.257 | 1.786 ± 0.209 | 0.441 |
| **Entropy Vert.** | 1.510 ± 0.456 | 1.656 ± 0.419 | 0.417 |
| **HR AP** | 1.473 ± 0.801 | 1.226 ± 0.569 | 0.420 |
| **HR Vert.** | 1.368 ± 0.781 | 0.904 ± 0.618 | 0.128 |
| **HR ML** | 2.940 ± 1.577 | 3.921 ± 3.093 | 0.214 |
| **CoM rms AP** | 0.020 ± 0.010 | 0.028 ± 0.014 | 0.115 |
| **CoM rms Vert.** | 0.010 ± 0.000 | 0.010 ± 0.000 | **0.009** |
| **CoM rms ML** | 0.011 ± 0.005 | 0.015 ± 0.012 | 0.161 |
| **Ampl. harm x** | 0.958 ± 0.283 | 0.895 ± 0.199 | 0.561 |
| **Ampl. harm y** | 0.935 ± 0.304 | 0.926 ± 0.333 | 0.942 |
| **Ampl. harm z** | 1.018 ± 0.317 | 1.004 ± 0.263 | 0.907 |
| **Width harm x** | 0.760 ± 0.225 | 0.693 ± 0.172 | 0.433 |
| **Width harm y** | 0.740 ± 0.200 | 0.742 ± 0.221 | 0.976 |
| **Width harm z** | 0.688 ± 0.185 | 0.596 ± 0.128 | 0.194 |
| **Slope harm x** | 1.552 ± 0.723 | 2.653 ± 3.138 | 0.075 |
| **Slope harm y** | 1.758 ± 0.877 | 3.533 ± 3.861 | **0.021** |
| **Slope harm z** | 2.868 ± 2.119 | 4.861 ± 4.722 | 0.081 |

The non-linear kinematic parameters (table 13) revealed that the centre of mass displacement along the vertical axis was statistically significant between the PD and atypical cohorts. Interestingly, the remaining parameters were different between both, but only the slope harm (y-axis) was significant and higher for the atypical group. Entropy AP, which was the most significant non-linear parameter on the previous comparison, was not significant in this case.

**Table 14** - Asymmetry parameters for PD (n=31) vs atypical group (n=8)

| | PD | Atypical | p-value |
|---|---|---|---|
| **Step time asymmetry [s]** | 0.036 ± 0.035 | 0.384 ± 0.936 | **0.038** |
| **Step length asymmetry [m]** | 0.071 ± 0.070 | 0.085 ± 0.072 | 0.610 |
| **Step width asymmetry [m]** | 0.030 ± 0.025 | 0.025 ± 0.019 | 0.602 |
| **Stride time asymmetry [s]** | 0.004 ± 0.006 | 0.336 ± 0.927 | **0.044** |
| **Stance fraction asymmetry [%]** | 1.969 ± 2.316 | 2.769 ± 2.662 | 0.404 |
| **Stance time asymmetry [s]** | 0.026 ± 0.036 | 0.094 ± 0.197 | 0.069 |
| **Swing fraction asymmetry [%]** | 1.969 ± 2.316 | 2.769 ± 2.662 | 0.404 |
| **Swing time asymmetry [s]** | 0.026 ± 0.035 | 0.094 ± 0.197 | 0.070 |
| **Double support asymmetry [%]** | 1.489 ± 1.840 | 3.343 ± 3.474 | 0.044 |

| | | | |
|---|---|---|---|
| **Double support time asymmetry [s]** | 0.018 ± 0.022 | 0.040 ± 0.037 | **0.037** |
| **Single support asymmetry [%]** | 1.970 ± 2.317 | 2.769 ± 2.661 | 0.404 |
| **Single support time asymmetry [s]** | 0.026 ± 0.034 | 0.092 ± 0.198 | 0.075 |
| **Pelvis list rom asymmetry [º]** | 0.137 ± 0.124 | 1.336 ± 3.336 | **0.045** |
| **Hip flexion rom asymmetry [º]** | 0.493 ± 0.284 | 2.107 ± 3.488 | **0.012** |
| **Hip adduction rom asymmetry [º]** | 0.303 ± 0.238 | 1.106 ± 1.645 | **0.010** |
| **Hip rotation rom asymmetry [º]** | 0.385 ± 0.212 | 1.870 ± 4.022 | **0.040** |
| **Knee angle rom asymmetry [º]** | 0.470 ± 0.440 | 1.768 ± 2.320 | **0.005** |
| **Ankle angle rom asymmetry [º]** | 0.355 ± 0.212 | 0.684 ± 0.541 | **0.009** |
| **Pelvis list mean vel asymmetry [cm/s]** | 0.081 ± 0.071 | 0.414 ± 0.650 | **0.006** |
| **Hip flexion mean vel asymmetry [cm/s]** | 0.570 ± 0.503 | 2.510 ± 4.034 | **0.010** |
| **Hip adduction mean vel asymmetry [cm/s]** | 0.268 ± 0.177 | 0.656 ± 0.563 | **0.002** |
| **Hip rotation mean vel asymmetry [cm/s]** | 0.399 ± 0.225 | 1.276 ± 2.405 | **0.045** |
| **Knee angle mean vel asymmetry [cm/s]** | 0.919 ± 0.710 | 3.392 ± 3.836 | **0.001** |
| **Ankle angle mean vel asymmetry [cm/s]** | 0.636 ± 0.537 | 1.586 ± 1.227 | **0.002** |
| **Speed asymmetry [m/s]** | 0.139 ± 0.136 | 0.181 ± 0.176 | 0.466 |

Lastly, the analysis of asymmetry when comparing the PD and atypical groups (table 14) displayed the highest significance. For instance, step time and stride time asymmetry were higher in the latter group, similarly to double support time asymmetry which was slightly increased compared to PD. Moreover, all asymmetries of angular gait-related features were statistically significant and increased for the atypical group in the differentiation, which includes all ranges of motion and mean velocities. On the other hand, speed asymmetry was slightly higher for the atypical cohort, but was not significant.

## 7.2. Section II – Correlations

**Table 15** - Pearson correlation between spatio-temporal kinematic parameters and PD motor UPDRS and disease duration (n=31)

| | Motor UPDRS | | Disease duration | |
|---|---|---|---|---|
| | r | p-value | r | p-value |
| **Cadence [steps/min]** | 0,044 | 0,815 | 0,026 | 0,889 |
| **Step time (worst side) [s]** | 0,009 | 0,961 | -0,02 | 0,916 |
| **Step length (worst side) [m]** | -0,109 | 0,561 | 0,072 | 0,701 |
| **Step width [m]** | -0,099 | 0,595 | 0,022 | 0,904 |
| **Step width (worst side) [m]** | -0,107 | 0,565 | 0,002 | 0,991 |
| **Stride time [s]** | -0,053 | 0,779 | -0,003 | 0,987 |
| **Stride time (worst side) [s]** | -0,051 | 0,787 | -0,01 | 0,956 |
| **Stride length [m]** | -0,151 | 0,417 | -0,074 | 0,693 |
| **Stance fraction (worst side) [%]** | -0,097 | 0,603 | 0,084 | 0,653 |
| **Stance time (worst side) [s]** | -0,064 | 0,732 | 0,01 | 0,956 |
| **Swing fraction (worst side) [%]** | 0,097 | 0,603 | -0,084 | 0,653 |
| **Swing time (worst side) [s]** | -0,014 | 0,941 | -0,103 | 0,58 |
| **Double support [%]** | -0,004 | 0,981 | 0,058 | 0,758 |
| **Double support (worst side) [%]** | 0,071 | 0,704 | 0,031 | 0,868 |
| **Double support time [s]** | -0,025 | 0,895 | 0,039 | 0,834 |
| **Double support time (worst side) [s]** | 0,035 | 0,854 | 0,029 | 0,878 |
| **Single support (worst side) [%]** | -0,051 | 0,785 | -0,033 | 0,86 |
| **Single support time (worst side) [s]** | -0,095 | 0,611 | -0,044 | 0,815 |

**Table 16** - Pearson correlation between speed and angular kinematic parameters and PD motor UPDRS and disease duration (n= 31)

| | Motor UPDRS | | Disease duration | |
|---|---|---|---|---|
| | r | p-value | r | p-value |
| **Speed [m/s]** | -0,099 | 0,598 | -0,028 | 0,881 |
| **Speed (worst side) [m/s]** | -0,059 | 0,752 | 0,095 | 0,61 |
| **Pelvis list rom (worst side) [º]** | 0,054 | 0,772 | 0,117 | 0,532 |
| **Hip flexion rom (worst side) [º]** | -0,196 | 0,291 | -0,012 | 0,951 |
| **Hip adduction rom (worst side) [º]** | -0,123 | 0,511 | -0,044 | 0,812 |
| **Hip rotation rom (worst side) [º]** | 0,055 | 0,768 | 0,142 | 0,448 |
| **Ankle angle rom (worst side) [º]** | -0,208 | 0,262 | 0,076 | 0,684 |

| | | | | |
|---|---|---|---|---|
| **Knee angle rom (worst side) [º]** | -0,008 | 0,967 | -0,019 | 0,919 |
| **Pelvis list mean vel (worst side) [cm/s]** | 0,085 | 0,648 | 0,033 | 0,859 |
| **Hip flexion mean vel (worst side) [cm/s]** | -0,12 | 0,519 | 0,016 | 0,932 |
| **Hip adduction mean vel (worst side) [cm/s]** | -0,069 | 0,712 | -0,067 | 0,719 |
| **Hip rotation mean vel (worst side) [cm/s]** | -0,061 | 0,744 | 0,084 | 0,652 |
| **Knee angle mean vel (worst side) [cm/s]** | 0,059 | 0,754 | -0,032 | 0,864 |
| **Ankle angle mean vel (worst side) [cm/s]** | -0,19 | 0,307 | 0,096 | 0,609 |

**Table 17** - Pearson correlation between non-linear kinematic parameters and PD motor UPDRS and disease duration (n = 31)

| | **Motor UPDRS** | | **Disease duration** | |
|---|---|---|---|---|
| | r | p-value | r | p-value |
| **Entropy AP** | 0,146 | 0,433 | 0,12 | 0,52 |
| **Entropy ML** | 0,117 | 0,531 | 0,277 | 0,132 |
| **Entropy Vert.** | -0,048 | 0,797 | -0,124 | 0,507 |
| **HR AP** | -0,109 | 0,558 | 0,088 | 0,639 |
| **HR Vert.** | 0,086 | 0,646 | 0,05 | 0,79 |
| **HR ML** | -0,228 | 0,216 | -0,156 | 0,401 |
| **CoM rms AP** | 0,032 | 0,865 | -0,053 | 0,776 |
| **CoM rms Vert.** | 0 | 1 | 0 | 1 |
| **CoM rms ML** | -0,027 | 0,885 | -0,261 | 0,156 |
| **Ampl harm x** | -0,191 | 0,304 | -0,184 | 0,322 |
| **Ampl harm y** | -0,051 | 0,786 | 0,088 | 0,638 |
| **Ampl harm z** | -0,178 | 0,339 | -0,267 | 0,146 |
| **Width harm x** | 0,092 | 0,624 | -0,143 | 0,444 |
| **Width harm y** | 0,005 | 0,978 | -0,073 | 0,698 |
| **Width harm z** | 0,014 | 0,941 | 0,1 | 0,594 |
| **Slope harm x** | -0,042 | 0,822 | -0,184 | 0,323 |
| **Slope harm y** | -0,278 | 0,13 | 0,197 | 0,289 |
| **Slope harm z** | 0,004 | 0,981 | -0,012 | 0,949 |

**Table 18** - Pearson correlation between kinematic parameters asymmetry and PD motor UPDRS and disease duration (n = 31)

| | **Motor UPDRS** | | **Disease duration** | |
|---|---|---|---|---|
| | r | p-value | r | p-value |
| **Step time asymmetry [s]** | 0,054 | 0,774 | -0,176 | 0,344 |
| **Step length asymmetry [m]** | -0,07 | 0,707 | -0,108 | 0,562 |
| **Step width asymmetry [m]** | 0,022 | 0,904 | -0,191 | 0,304 |
| **Stride time asymmetry [s]** | 0,042 | 0,822 | 0,33 | 0,07 |
| **Stance fraction asymmetry [%]** | 0,02 | 0,914 | -0,086 | 0,644 |
| **Stance time asymmetry [s]** | 0,003 | 0,988 | -0,082 | 0,66 |
| **Swing fraction asymmetry [%]** | 0,02 | 0,914 | -0,086 | 0,644 |
| **Swing time asymmetry [s]** | -0,019 | 0,919 | -0,103 | 0,582 |
| **Double support asymmetry [%]** | 0,049 | 0,795 | -0,225 | 0,225 |
| **Double support time asymmetry [s]** | 0,073 | 0,695 | -0,194 | 0,295 |
| **Single support asymmetry [%]** | 0,02 | 0,917 | -0,086 | 0,644 |
| **Single support time asymmetry [s]** | -0,004 | 0,981 | -0,096 | 0,609 |
| **Pelvis list rom asymmetry [º]** | 0,237 | 0,2 | 0,079 | 0,674 |
| **Hip flexion rom asymmetry [º]** | 0,069 | 0,712 | 0,017 | 0,929 |
| **Hip adduction rom asymmetry [º]** | 0,07 | 0,71 | 0,119 | 0,525 |
| **Hip rotation rom asymmetry [º]** | -0,46 | **0,009** | -0,098 | 0,602 |
| **Knee angle rom asymmetry [º]** | 0,051 | 0,786 | -0,11 | 0,555 |
| **Ankle angle rom asymmetry [º]** | 0,019 | 0,92 | 0,08 | 0,671 |
| **Pelvis list mean vel asymmetry [cm/s]** | -0,106 | 0,569 | -0,198 | 0,285 |
| **Hip flexion mean vel asymmetry [cm/s]** | -0,426 | **0,017** | -0,234 | 0,206 |
| **Hip adduction mean vel asymmetry [cm/s]** | -0,009 | 0,961 | -0,168 | 0,366 |
| **Hip rotation mean vel asymmetry [cm/s]** | -0,112 | 0,548 | -0,178 | 0,337 |
| **Knee angle mean vel asymmetry [cm/s]** | -0,244 | 0,187 | -0,139 | 0,456 |
| **Ankle angle mean vel asymmetry [cm/s]** | -0,355 | **0,05** | -0,123 | 0,511 |
| **Speed asymmetry [m/s]** | -0,013 | 0,943 | -0,179 | 0,335 |

We also investigated the association between the acquired gait-related parameters and some of the patient's clinical data such as motor UPDRS and disease duration (tables 15-18). This was done through the Pearson correlation coefficient (r) with statistical significance at $p<0.005$. This analysis showed that no spatio-temporal, speed/angular or non-linear kinematic parameter displayed significant statistical correlation, with weak correlation ($r=0.2$) being the maximum registered for parameters such as HR ML and slope harm (y) with motor UPDRS, and amplitude harm (z) with disease duration. On the other hand, analysis of asymmetry revealed that hip rotation RoM asymmetry, hip flexion mean velocity asymmetry and ankle angle mean velocity asymmetry presented significant correlation, all with motor UPDRS. No asymmetric parameter was significantly correlated with disease duration.

### 7.3. Section III – Machine Learning approach

#### 7.3.1. Classifying Controls vs Ill (PD + atypical)

The first approach consisted of classifying the control group versus the remaining study subjects (PD + atypical), as a means of understanding how accurately such a model could correctly predict true negatives and true positives. A random forest classifier was used as mentioned in materials and methods and the results are presented in the form of performance scores resume (with special focus on classification accuracy) and confusion matrix.

**Table 19** - Performance scores for Random Forest when classifying controls (n=31) vs ill (n=39), total (n=70)

| **Random Forest**<br><br>**Controls vs Ill (PD + atypical)** | |
|---|---|
| **Scores** | |
| **CA** | 0.829 |
| **Precision** | 0.829 |
| **Recall** | 0.829 |
| **F1** | 0.828 |

**Table 20** - Confusion matrix for Random Forest when classifying controls (n=31) vs ill (n=39), total (n=70)

| | | **Predicted** | |
|---|---|---|---|
| | | Control | Ill |
| **Actual** | Control | 24 | 7 |
| | Ill | 5 | 34 |

Classification of subjects on the control group (n=31) vs ill group (n=39) using a random forest with 162 spatiotemporal kinematic features and 10-fold cross validation (table 19) yielded a CA of 0.829 (82.9%). All other performance scores were the same except for F1 (0.828 = 82.8%). Confusion matrix (table 20) results showed that the number of correctly predicted cases were 58 (true negative (controls) = 24, true positive (ill) = 34) and incorrectly predicted were 12 (false negative = 5 (parkinsonian cases predicted as controls), false positive = 7 (controls cases predicted as parkinsonism)).

#### 7.3.2. Classifying PD vs atypical

Next, classification of PD versus atypical parkinsonism subjects was conducted. In this case the objective was to assess if the model could, within the parkinsonian group, distinguish between Parkinson's disease and the atypical parkinsonian syndromes. The previous random forest model using 10-fold cross validation was implemented without any settings changes and the results are again presented in the form of performance scores and confusion matrix. In this

case, true negatives are PD subjects who are predicted as PD, true positives are atypical subjects predicted as atypical, false negatives are atypical subjects who are predicted as PD and false positives are PD subjects who are predicted as atypical. Since the sample size for the atypical group is considerably smaller (31 PD vs 8 atypical), the Parkinson's disease cohort was previously split into three groups of eight subjects each and one group of seven subjects, with the classifier being tested individually for each group combination. The results for this analysis (i.e. classification scores and confusion matrix) are presented as average of all tests.

**Table 21** - Performance scores for Random Forest when classifying PD (n=31) vs atypical (n=8), total (n=39)

| **Random Forest** | |
|---|---|
| **PD vs atypical** | |
| **Scores** | |
| **CA** | 0.763 |
| **Precision** | 0.766 |
| **Recall** | 0.763 |
| **F1** | 0.762 |

**Table 22** - Confusion matrix for Random Forest when classifying PD (n=31) vs atypical (n=8), total (n=39)

| | | **Predicted** | |
|---|---|---|---|
| | | PD | Atypical |
| **Actual** | PD | 6 | 2 |
| | Atypical | 2 | 6 |

Random forest results using the same number of spatiotemporal kinematic features (n=162) show a CA of 0.763 (76.3%) when classifying the PD cohort (n=31) against the atypical cohort (n=8). The remaining scores go as follows: precision (0.766 = 76.6%), recall (0.763 = 76.3%) and F1 (0.762 = 76.2%), table 21. Confusion matrix results (table 22) reveal that 12 cases were correctly predicted (true negative (PD) = 6, true positive (atypical) = 6) and only 4 were incorrectly predicted (false negative = 2, atypical cases predicted as PD, false positive = 2, PD cases predicted as atypical).

### 7.4. Section IV - Finger tapping analysis

As mentioned before, we collected finger tapping movement data from all subjects that performed gait and postural tests. The 9 degrees of freedom IMU measured acceleration, angular velocity and magnetic orientation in all three axes, but because of the orientation of the sensor in relation to the finger, the y-axis of the gyroscope presents a good representation of the movement performed (as seen in figure 13 the blue square represents the antenna which was placed right above the finger nail).

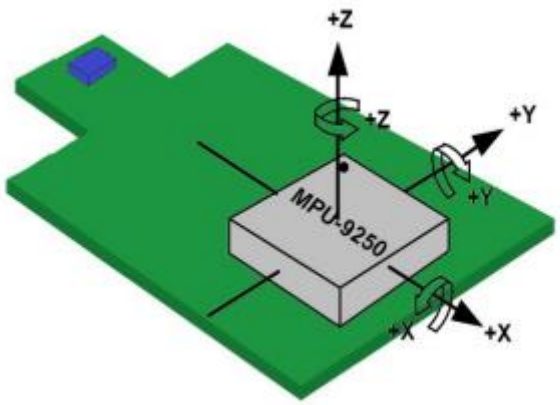


**Figure 13** - Gyroscope orientation of its x, y and z axis

Here, we will show an example of a finger tapping test for controls (figure 14), PD (figure 15) and atypical (figure 16) subjects, based on the readings of the gyroscope y-axis.

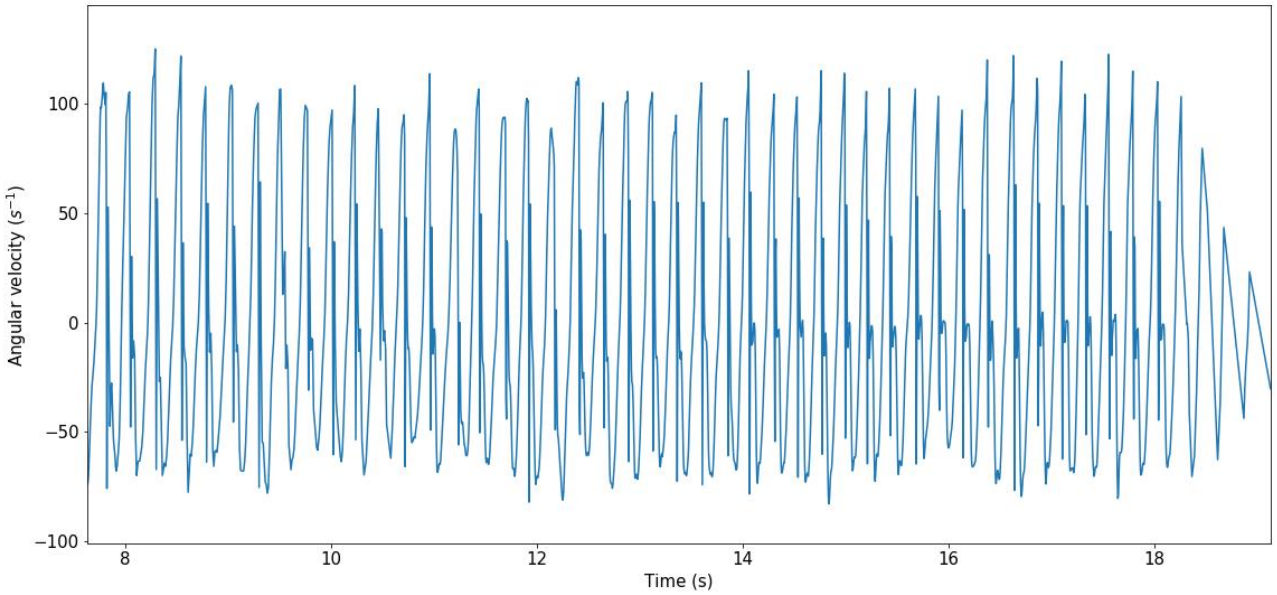


**Figure 14** - Example of a 10 second control finger tapping test based on the gyroscope y-axis readings

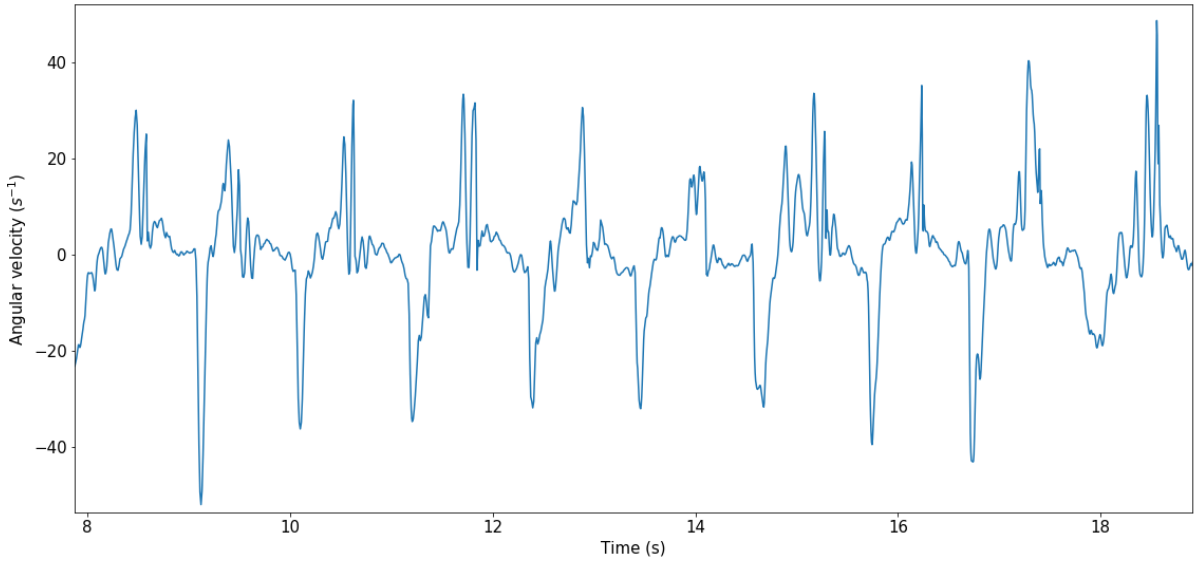


**Figure 15** - Example of a 10 second PD finger tapping test based on the gyroscope y-axis readings

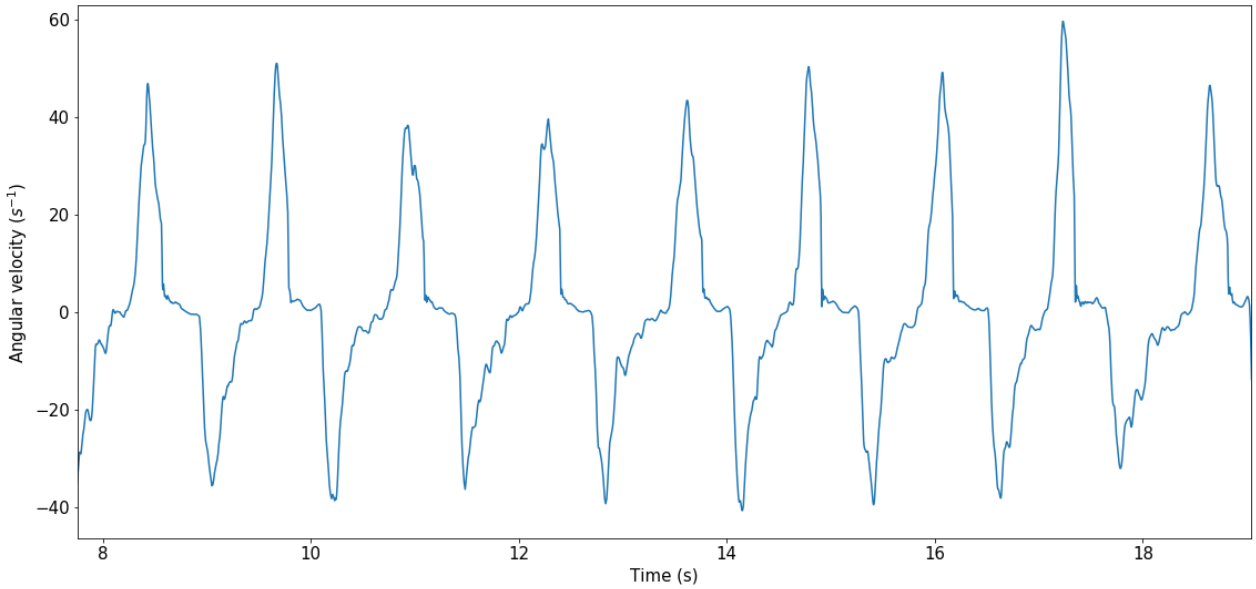


**Figure 16** - Example of a 10 second atypical finger tapping test based on the gyroscope y-axis readings

From a direct visualization of these examples, we can see some differences between the groups. The clearest difference is that controls are able to perform (on average) more finger tapping cycles than PD and atypical subjects in the same time period. Eventually, we want to extract several kinematic features from these tests, such as speed, tap cycle duration and amplitude, as well as variation of tapping metrics to assess the performance of the test during its time span. For that we will be analysing the signals from all 9 DOF and not only the gyroscope y-axis, slice finger tap cycles one by one and extract their features. Figure 17 gives an example of the metrics we want to further explore in this analysis.

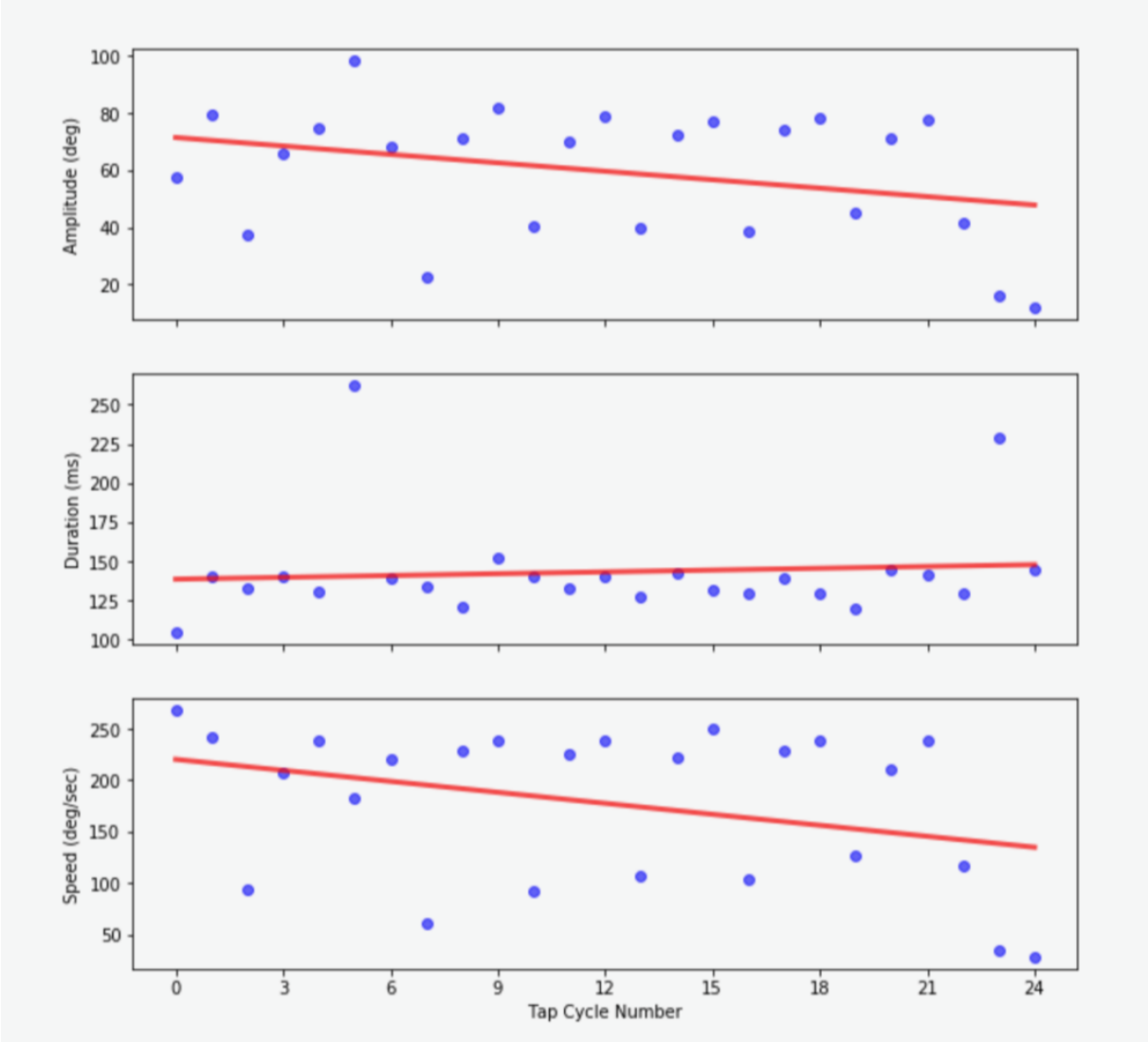


**Figure 17** - Example of metrics to be extracted from finger tapping tests. In this case amplitude, duration and speed (function of number of tap cycles, in blue), with respective linear regressions (in red) to assess variation for the duration of the test.

## 8. Discussion

We've studied the role of inertial-sensor based lower limb kinematics in the differential diagnosis of parkinsonism. In the first analysis we wanted to check if there were significant kinematic parameters that differed between the control group and the parkinsonian group as a whole (PD + atypical subjects). Analysing the first set of parameters (spatio-temporal), we can see that generally, step/stride length and time-wise features and percentages of gait were higher in the parkinsonian group compared to controls. For instance, stride length and step length were the most significantly reduced in the parkinsonian group, similarly to what Raccagni and colleagues found [51]. Also, as reported before [49], double support was increased in parkinsonian patients, which may come as a result of instable gait that is usually present in this group, as subjects need to better support themselves before starting a new gait cycle. The second group of features where velocities and angles are assessed, speed (and speed worst-side) were severely affected in the parkinsonian group – this has been also shown before by several studies and is easily detectable when one observes a parkinsonian patient walk, for its characterized by slow, pondered movements. Notably, hip flexion in this group were also significantly impaired as both range of motion and mean velocity were reduced compared to controls. Interestingly, this goes according with previous literature which states that Parkinson's patients have high prevalence to develop conditions such as osteoporosis and low bone mineral density, making them prone to suffer hip fractures [58]. Although more investigation needs to be done in this matter, one could hypothesize that these conditions could lead to lower biomechanical performance of the hip joint, consequently reducing its range of motion and velocity. It's also worth mentioning that other angular parameters were significantly reduced in the parkinsonian cohort, such as the knee range of motion and mean velocity, and the ankle mean velocity, which together give the idea that these subjects suffer from reduced capability of those joints. Analysis of non-linear features revealed little to no significance, as only entropy AP and vertical harmonic ratio was different between the groups. Finally, asymmetry showed no significance, and contrarily to what would be anticipated, the control group displayed higher step width asymmetry, which one would expect to be more pronounced on the parkinsonian group.

In the second analysis we tested how to better distinguish PD from atypical parkinsonian patients. Double support time (both average and worst-side) and consequently percentage of gait were clearly increased in the atypical group. This suggests that subjects suffering from atypical parkinsonian disorders such as PSP and MSA will display higher gait instability and will find themselves in need of carefully supporting each step. This is to be expected because PSP patients in particular (which represent most of our atypical group) suffer from early postural instability and falls. Moreover, analysis of angular parameters revealed a significant decreased in biomechanical performance of the ankle joint on the atypical parkinsonian cohort, marked by the reduced range of motion and mean velocity compared to PD. This suggests that for the atypical cohort, the ankle joint might suffer from an underlying mechanism that reduces its capabilities, or that it might have to do with the instability these patients experience, overall reducing the ankles mobility. Anyway, further research should be conducted in order to assess this question. It should be noted that speed was reduced for the atypical group, but was not statistically significant. Moving on to the non-linear parameters, the vertical displacement of center of mass was significant when distinguishing between both groups, possibly representing that the atypical cohort suffers from higher instability during gait. Finally, we believe that one of the most interesting findings of this work

was the overall asymmetry present in the atypical parkinsonian cohort. Asymmetry was higher in this group for every measured parameter and in some cases more than double or triple of that observed in the PD group. Most of the asymmetric features revealed statistical significance for distinction between both groups, with all angular asymmetries being significant for all joints movements and velocities. It is worth mentioning the knee and ankle angle mean velocity, hip adduction mean velocity and knee and ankle range of motion. With our results, we can safely say that gait in atypical parkinsonian syndromes suffers from high asymmetry, much higher than that seen in PD and, obviously, controls.

The analysis performed next consisted of correlating the acquired kinematic data and the patients' clinical data from the PD cohort in order to see if inertial sensors could capture what the neurological community think is relevant for assessment of PD, and it was done based on the motor UPDRS and disease duration. Correlation with motor UPDRS revealed that only three metrics of angular asymmetry were significantly correlated, displaying negative association with this clinical feature. These were hip rotation range of motion asymmetry with the strongest negative association, followed by hip flexion mean velocity asymmetry and ankle angle mean velocity asymmetry. It was an interesting finding and it means that the higher motor UPDRS, the lower angular asymmetric behaviour of Parkinson's disease subjects, possibly meaning that this cohort displays less asymmetric angles during gait as their motor UPDRS increases. This makes sense because with disease progression, subjects become more neurologically degenerated with similar dopamine depletion on both sides, thus reducing asymmetry. Association with disease duration was also performed and we found that no gait-related kinematic parameter showed significant association with this clinical feature, possibly meaning that inertial sensors are not able to detect significant kinematic changes based on the subjects disease duration. Although more research has to be done in this matter, these are important findings which suggest that asymmetry reduces at more advanced disease stages in PD. One could hypothesize that a more pronounced stage of short-stepped gait leaves less room for variability between both sides, thus reducing asymmetry based on the symmetric depletion of dopamine.

We believe our machine learning approach yielded positive results. We wanted to see if using the available kinematic parameters and a relatively standard random forest algorithm, we could create a model to classify the subjects in two levels: first classify controls vs the parkinsonian group (PD + atypical) and then classify subjects within the parkinsonian group, that is PD vs atypical. In the first approach the model was able to classify with an accuracy of 82.9%, with only 5 false negative classified cases, which in theory would be the group that we would like to reduce the most, because those are the cases that we though were controls, but were in fact ill (with either PD or any other atypical parkinsonism). In the second level of classification, our model also performed positively, with an accuracy of 76.3%. It's worth mentioning that we divided our PD group like mentioned before in order to equal the size of the atypical cohort, and ran the classification model 4 times. The average results showed that 6 out of 8 PD cases were correctly predicted, and the same goes for the atypical group. We think that for the sample size the results were good, and probably mostly based on the asymmetry found on the latter. Anyway, we can safely say that future work should be performed with a larger atypical cohort in order to increase model accuracy.

A word should also be given about the clinical application of inertial sensors. During this work, this technology was very simple to implement, with a straight forward protocol that

allows patients to comfortably perform the required tests. All that was needed was a kit of sensors like the one we used, and someone to equip/unequip the subjects and collect the data while the test was being performed. Compared to the imaging techniques previously mentioned used for assessment of differential diagnosis between PD and atypical parkinsonism, which in many cases require expensive equipment, highly specialized personnel and infrastructures, prior subject preparation (up to a few hours i.e. DaTscan), and sometimes posing potential side effects, the inertial sensor technology is safe to use (since the patients are only asked to walk), and apart from the mentioned prerequisites, it should be performed on an empty, unobstructed corridor that requires no special inspection. This technology is definitely easy to implement on a daily basis, and supported by the scientific evidence we provided, we believe it should be implemented as soon as possible in this field.

Lastly, we must mention that ongoing work is being developed in the analysis of finger tapping tests and postural stability. We are hopeful that those results will give us important kinematic features that will not only help us understand where these diseases are different, but potentially assist our machine learning models and increase differential diagnosis accuracy.

## 9. Conclusions

We believe the main objectives of this work were achieved. Answering the previously posed questions, we were able to provide many gait-related parameters where Parkinson's disease and atypical parkinsonian subjects differ from a kinematic standpoint. More precisely, we hypothesize that atypical parkinsonian subjects develop an instable gait where asymmetry is highly pronounced – not only that, they differ from PD in many other parameters.

Finally, we believe that inertial technology can help in the differential diagnosis between Parkinson's disease and atypical parkinsonism based on the results provided, where we show that atypical parkinsonism is marked by high gait variability compared to Parkinson's disease, and which can be captured using miniature inertial sensors leveraged by biomechanical models. Not only that, but it's a technology that offers many advantages compared with the current techniques, and supported by machine learning it can enhance diagnostic accuracy in order to improve patient prognostic and treatment, overall increasing the efficiency of health care resources and patient quality of life. Although research still needs to be performed in this matter in order to accurately say where these syndromes differ from one another and to improve machine learning models performance, we believe that, with the right investment, this technology is one step away from seeing clinical application.

## Bibliography


[1] L. V. Kalia and E. L. Anthony, “Parkinson’s Disease,” *Lancet*, vol. 386, no. 9996, pp. 896–912, 2015.

[2] A. Antonini and Y. Bordelon, “Radiological Biomarkers for Diagnosis in PSP : Where Are We and Where Do We Need to Be ?,” vol. 00, no. 00, pp. 1–17, 2017.

[3] D. R. S. Ba *et al.*, “F-flortaucipir tau PET distinguishes established progressive supranuclear palsy from controls and Parkinson ’ s disease : A multicenter study,” pp. 2–44.

[4] M. Politis, Roussakis, and P. Piccini, “Clinical utility of DaTscan™ (123I-Ioflupane Injection) in the diagnosis of Parkinsonian Syndromes,” *Degener. Neurol. Neuromuscul. Dis.*, p. 33, 2013.

[5] L. Brognara, P. Palumbo, B. Grimm, and L. Palmerini, “Assessing Gait in Parkinson’s Disease Using Wearable Motion Sensors: A Systematic Review,” *Diseases*, vol. 7, no. 1, p. 18, 2019.

[6] J. Parkinson, “An essay on the shaking palsy [reprint of monograph published by Sherwood, Neely, and Jones, London, 1817],” *J. Neuropsychiatry Clin. Neurosci.*, vol. 14, no. 2, pp. 223–236, 2002.

[7] C. G. Goetz, “The history of Parkinson’s disease: early clinical descriptions and neurological therapies.,” *Cold Spring Harb. Perspect. Med.*, vol. 1, no. 1, p. a008862, 2011.

[8] A. Yarnall, N. Archibald, and D. Burn, “Parkinson’s Disease,” *Medicine (Baltimore).*, vol. 40, no. 10, pp. 529–535, 2012.

[9] L. Hirsch, N. Jette, A. Frolkis, T. Steeves, and T. Pringsheim, “The Incidence of Parkinson’s Disease: A Systematic Review and Meta-Analysis,” *Neuroepidemiology*, vol. 46, no. 4, pp. 292–300, 2016.

[10] S. K. Van Den Eeden *et al.*, “Incidence of Parkinson’s disease: variation by age, gender, and race/ethnicity.,” *Am. J. Epidemiol.*, vol. 157, no. 11, pp. 1015–22, 2003.

[11] L. De Lau and M. Breteler, “Epidemiology of Parkinson’s disease,” *Lancet Neurol.*, vol. 5, no. 6, pp. 525–535, 2006.

[12] T. Pringsheim, N. Jette, A. Frolkis, and T. D. L. Steeves, “The prevalence of Parkinson’s disease: a systematic review and meta-analysis.,” *Mov. Disord.*, vol. 29, no. 13, pp. 1583–90, 2014.

[13] C. M. Lill, “Genetics of Parkinson disease,” *Mol. Cell. Probes*, no. 30, pp. 386–396, 2016.

[14] H. M. Gao and J. S. Hong, “Gene-environment interactions: Key to unraveling the mystery of Parkinson’s disease,” *Prog. Neurobiol.*, vol. 94, no. 1, pp. 1–19, 2011.

[15] N. Ball, W.-P. Teo, S. Chandra, and J. Chapman, “Parkinson’s Disease and the Environment,” *Front. Neurol.*, vol. 10, no. March, p. 218, 2019.

[16] Y. H. Chuang *et al.*, “Gene-Environment Interaction in Parkinson’s Disease: Coffee, ADORA2A, and CYP1A2,” *Neuroepidemiology*, vol. 47, no. 3–4, pp. 192–200, 2017.

[17] J. Knierim, “Neuroscience: Basal Ganglia,” *Neuroscience*, 2000. [Online]. Available: https://nba.uth.tmc.edu/neuroscience/m/s3/chapter04.html. [Accessed: 30-Apr-2019].

[18] M. Goedert, M. G. Spillantini, K. Del Tredici, and H. Braak, “100 years of Lewy pathology,” *Nat. Rev. Neurol.*, vol. 9, no. 1, pp. 13–24, 2013.

[19] M. H. Polymeropoulos *et al.*, “Mutation in the α-synuclein gene identified in families with Parkinson’s disease,” *Science (80-. ).*, vol. 276, no. 5321, pp. 2045–2047, 1997.

[20] R. A. Crowther, M. Hasegawa, M. G. Spillantini, R. Jakes, and M. Goedert, “-Synuclein in filamentous inclusions of Lewy bodies from Parkinson’s disease and dementia with Lewy bodies,” *Proc. Natl. Acad. Sci.*, vol. 95, no. 11, pp. 6469–6473, 2002.

[21] H. Braak, K. Del, U. Rüb, R. A. I. De Vos, E. N. H. Jansen, and E. Braak, “Staging of brain pathology related to sporadic Parkinson’s disease,” *Neurobiol. Aging*, vol. 24, pp. 197–211, 2003.

[22] L. V. Kalia, S. K. Kalia, P. J. McLean, A. M. Lozano, and A. E. Lang, “A-Synuclein Oligomers and Clinical Implications for Parkinson Disease,” *Ann. Neurol.*, vol. 73, no. 2, pp. 155–169, 2013.

[23] D. J. Irwin, V. M. Y. Lee, and J. Q. Trojanowski, “Parkinson’s disease dementia: Convergence of α-synuclein, tau and amyloid-β pathologies,” *Nat. Rev. Neurosci.*, vol. 14, no. 9, pp. 626–636, 2013.

[24] A. J. Noyce *et al.*, “Meta-analysis of early nonmotor features and risk factors for Parkinson disease,” *Ann. Neurol.*, vol. 72, no. 6, pp. 893–901, 2012.

[25] J. Jankovic, “Parkinson’s disease: clinical features and diagnosis,” *J. Neurol. Neurosurg. Psychiatry*, vol. 79, pp. 368–376, 2008.

[26] S. G. Reich and J. M. Savitt, “Parkinson’s Disease,” *Med. Clin. North Am.*, vol. 103, no. 2, pp. 337–350, 2019.

[27] National Institute of Neurological Disorders and Stroke - Office of Communications and Public Liaison, “Tremor Fact Sheet,” 2019. [Online]. Available: https://www.ninds.nih.gov/Disorders/Patient-Caregiver-Education/Fact-Sheets/Tremor-Fact-Sheet. [Accessed: 13-Jun-2019].

[28] D. R. Williams, H. C. Watt, and A. J. Lees, “Predictors of falls and fractures in bradykinetic rigid syndromes: A retrospective study,” *J. Neurol. Neurosurg. Psychiatry*, vol. 77, no. 4, pp. 468–473, 2006.

[29] E. Broussolle, P. Krack, S. Thobois, J. Xie-Brustolin, P. Pollak, and C. G. Goetz, “Contribution of Jules Froment to the study of parkinsonian rigidity,” *Mov. Disord.*, vol. 22, no. 7, pp. 909–914, 2007.

[30] C. G. Goetz *et al.*, “Movement Disorder Society-Sponsored Revision of the Unified Parkinson ’ s Disease Rating Scale ( MDS-UPDRS ): Scale Presentation and Clinimetric Testing Results,” vol. 23, no. 15, pp. 2129–2170, 2008.

[31] M. Stamelou, N. Giagkou, and G. U. Höglinger, “One decade ago, one decade ahead in progressive supranuclear palsy,” *Mov. Disord.*, p. mds.27788, 2019.

[32] G. G. Kovacs, “Invited review: Neuropathology of tauopathies: Principles and practice,” *Neuropathol. Appl. Neurobiol.*, vol. 41, no. 1, pp. 3–23, 2015.

[33] G. U. Höglinger *et al.*, “Rational therapeutic approaches to progressive supranuclear palsy,” *Brain*, vol. 133, no. 6, pp. 1578–1590, 2010.

[34] D. R. Williams *et al.*, “Characteristics of two distinct clinical phenotypes in pathologically proven progressive supranuclear palsy: Richardson’s syndrome and PSP-parkinsonism,” *Brain*, vol. 128, no. 6, pp. 1247–1258, 2005.

[35] H. Ling, L. A. Massey, A. J. Lees, P. Brown, and B. L. Day, “Hypokinesia without decrement distinguishes progressive supranuclear palsy from Parkinson’s disease,” *Brain*, vol. 135, no. 4, pp. 1141–1153, 2012.

[36] H. Ling, “Clinical Approach to Progressive Supranuclear Palsy,” *J. Mov. Disord.*, vol. 9, no. 1, pp. 3–13, 2016.

[37] N. K. Magdalinou *et al.*, “A panel of nine cerebrospinal fluid biomarkers may identify patients with atypical parkinsonian syndromes,” *J. Neurol. Neurosurg. Psychiatry*, vol. 86, no. 11, pp. 1240–1247, 2015.

[38] K. A. Jellinger, “Multiple system atrophy: An oligodendroglioneural synucleinopathy,” *J. Alzheimer’s Dis.*, vol. 62, no. 3, pp. 1141–1179, 2018.

[39] J. Q. Trojanowski and T. Revesz, “Proposed neuropathological criteria for the post mortem diagnosis of multiple system atrophy,” *Neuropathol. Appl. Neurobiol.*, vol. 33, no. 6, pp. 615–620, 2007.

[40] S. Koga *et al.*, “When DLB, PD, and PSP masquerade as MSA: an autopsy study of 134 patients.,” *Neurology*, vol. 85, no. 5, pp. 404–12, 2015.

[41] G. Treglia, A. Stefanelli, E. Cason, F. Cocciolillo, D. Di Giuda, and A. Giordano, “Diagnostic performance of iodine-123-metaiodobenzylguanidine scintigraphy in differential diagnosis between Parkinson’s disease and multiple-system atrophy: A systematic review and a meta-analysis,” *Clin. Neurol. Neurosurg.*, vol. 113, no. 10, pp. 823–829, 2011.

[42] N. K. Focke *et al.*, “Differentiation of typical and atypical Parkinson syndromes by quantitative MR imaging,” *Am. J. Neuroradiol.*, vol. 32, no. 11, pp. 2087–2092, 2011.

[43] J. McKinley, M. O’Connell, M. Farrell, and T. Lynch, “Normal dopamine transporter imaging does not exclude multiple system atrophy,” *Park. Relat. Disord.*, vol. 20, no. 8, pp. 933–934, 2014.

[44] A. D. Korczyn, “Vascular parkinsonism—characteristics, pathogenesis and treatment,” *Nat. Publ. Gr.*, pp. 1–8, 2015.

[45] F. Brigo, A. Matinella, R. Erro, and M. Tinazzi, “[ $^{123}$ I ] FP-CIT SPECT ( DaTSCAN ) may be a useful tool to differentiate between Parkinson ’ s disease and vascular or drug-induced parkinsonisms : a meta-analysis,” pp. 1–10, 2014.

[46] W. Tao, T. Liu, R. Zheng, and H. Feng, “Gait Analysis Using Wearable Sensors,” *Sensors*, vol. 12, pp. 2255–2283, 2012.

[47] R. Caldas, M. Mundt, W. Potthast, F. Buarque, and D. L. Neto, “Gait & Posture A systematic review of gait analysis methods based on inertial sensors and adaptive algorithms,” *Gait Posture*, vol. 57, no. February, pp. 204–210, 2017.

[48] J. C. M. Schlachetzki *et al.*, “Wearable sensors objectively measure gait parameters in Parkinson ’ s disease,” *PLoS One*, pp. 1–18, 2017.

[49] C. Caramia *et al.*, “IMU-Based Classification of Parkinson’s Disease from Gait: A Sensitivity Analysis on Sensor Location and Feature Selection,” *IEEE J. Biomed. Heal. Informatics*, vol. 22, no. 6, pp. 1765–1774, 2018.

[50] C. Curtze, J. G. Nutt, P. Carlson-kuhta, M. Mancini, and F. B. Horak, “Levodopa Is a Double-Edged Sword for Balance and Gait in People With Parkinson ’ s Disease Parkinson and Movement Disorder Society,” *Mov. Disord.*, vol. 30, no. 10, pp. 1361–1370, 2015.

[51] C. Raccagni *et al.*, “Sensor-based gait analysis in atypical parkinsonian disorders,” *Wiley - Brain Behav.*, no. February, pp. 1–9, 2018.

[52] V. Bobic, M. Djuric-Jovicic, N. Dragasevic, M. B. Popovic, V. s. Kostic, and G. Kvascev, “An Expert System for Quantification of Bradykinesia,” *Sensors*, vol. 19, no. 11, 2019.

[53] T. Yiu, “Understanding Random Forest,” *Towards Data Science*. 21-Sep-2019.

[54] R. Pal, *Predictive Modeling of Drug Sensitivity*. 2017.

[55] J. Brownlee, “A Gentle Introduction to k-fold Cross-Validation,” *Machine Learning Mastery*. 23-Sep-2018.

[56] C. L. Tomlinson, R. Stowe, S. Patel, C. Rick, R. Gray, and C. E. Clarke, “Systematic review of levodopa dose equivalency reporting in Parkinson’s disease,” *Mov. Disord.*, vol. 25, no. 15, pp. 2649–2653, 2010.

[57] A. Cervantes-Arriaga, M. Rodríguez-Violante, A. Villar-Velarde, and T. Corona, “Calculo de unidades de equivalencia de levodopa en enfermedad de Parkinson,” *Arch. Neurociencias*, vol. 14, no. 2, pp. 116–119, 2009.

[58] A. R. Coomber, Z. Alshameeri, F. Masia, F. Mela, and M. J. Parker, “Hip fractures and Parkinson’s disease: a case series,” *Injury*, vol. 48, no. 12, pp. 2730–2735, 2017.